A thermohydraulic model that represents the current configuration of the SAFARI-1 secondary cooling system

---

Ewan
Huisamen

Volume I

2015

A thermohydraulic model that represents the current configuration of the SAFARI-1 secondary cooling system

---

by

Ewan Huisamen

26043409

Submitted in partial fulfilment of the requirements for the degree

MASTER OF ENGINEERING

in the

Department of Mechanical and Aeronautical Engineering of the Faculty of Engineering, Built Environment and Information Technology

University of Pretoria

Volume I

Volume I: Chapter 1 to 7

Volume II: Appendix I to VII

2015

UNIVERSITEIT VAN PRETORIA
UNIVERSITY OF PRETORIA
YUNIBESITHI YA PRETORIA

Synopsis

Title:	A thermohydraulic model that represents the current configuration of the SAFARI-1 secondary cooling system
Author:	Ewan Huisamen (26043409)
Supervisors:	Prof JFM Slabber and Prof JP Meyer
	Department: Mechanical and Aeronautical
	Engineering University: University of Pretoria
Degree:	Master of Engineering (Mechanical Engineering)

This document focuses on the procedure and results of creating a thermohydraulic model of the secondary cooling system of the SAFARI-1 research reactor at the Pelindaba facility of the South African Nuclear Energy Corporation (Necsa) to the west of Pretoria, South Africa.

The secondary cooling system is an open recirculating cooling system that comprises an array of parallel-coupled heat exchangers between the primary systems and the main heat sink system, which consists of multiple counterflow-induced draught cooling towers.

The original construction of the reactor was a turnkey installation, with no theoretical/technical support or verifiability. The design baseline is therefore not available and it is necessary to reverse-engineer a system that could be modelled and characterised.

For the nuclear operator, it is essential to be able to make predictions and systematically implement modifications to improve system performance, such as to understand and modify the control system. Another objective is to identify the critical performance areas of the thermohydraulic system or to determine whether the cooling capacity of the secondary system meets the optimum original design characteristics.

The approach was to perform a comprehensive one-dimensional modelling of all the available physical components, which was followed by using existing performance data to verify the accuracy and validity of the developed model. Where performance data is not available, separate analysis through computational fluid dynamics (CFD) modelling is performed to generate the required inputs.

The results yielded a model that is accurate within 10%. This is acceptable when

compared to the variation within the supplied data, generated and assumed alternatives, and when considering the compounding effect of the large amount of interdependent components, each with their own characteristics and associated performance uncertainties.

The model pointed to potential problems within the current system, which comprised either an obstruction in a certain component or faulty measuring equipment. Furthermore, it was found that the current spray nozzles in the cooling towers are underutilised. It should be possible to use the current cooling tower arrangement to support a similar second reactor, although slight modifications would be required to ensure that the current system is not operated beyond its current limits. The interdependent nature of two parallel systems and the variability of the conditions that currently exist would require a similar analysis as the current model to determine the viability of using the existing cooling towers for an additional reactor.

Keywords: *thermohydraulic model, nuclear, one-dimensional modelling, computational fluid dynamics*

Acknowledgements

I would like to thank the following people:

- Mr Ari Hatting (Necsa) for his prompt and effective assistance at all times.
- Dr Andre van Heerden (former Necsa employee) for his undying enthusiasm and commitment to the project.
- Keith Railton (former Esteq employee) for turning a world of Greek into English.
- Prof JFM Slabber (University of Pretoria) for unfailing support, knowledge, friendship and a love for the nuclear fraternity.
- My family, who are the *raison d'être* for this thesis.

Table of contents

Volume I

VOLUME II

List of figures

List of tables

Nomenclature

List of symbols

Symbol	Description	Unit
η_e	Electrical efficiency	-
η_h	Hydraulic efficiency	-
η_m	Mechanical efficiency	-
f	Frequency in Hertz	Hz
H_f	Heat fraction	-
p	Number of poles	-
$\dot{P}$	Total power delivered	W
$\dot{P}_e$	Electrical power supplied	w
Q	Flow rate	l/s
v	Flow velocity	m/s

Greek symbols

Symbol	Description	Unit
α	The obtuse angle between the Leg A inlet and Leg C outlet of the Y-strainer	°
β	The obtuse angle between the Leg B inlet and Leg C outlet of the Y-strainer	°
λ_1, λ_2	Loss coefficients in Vazsonyi's formulae	-

Subscripts and superscripts

Symbol	Description	Unit
c	Cold	-
h	Hot	-
in	As found at the inlet	-
max	Maximum	-
min	Minimum	-
out	As found at the outlet	-

List of abbreviations

The -XXXX designator refers to a unique number in the piping and instrumentation diagram.

Abs	Absolute (value)
API	American Petroleum Industry (Codes and Standards)
Av	Average (value)
CAD	Computer-aided design
CFD	Computational fluid dynamics
C-*XXXX*	Ball strainer
E-NTU	Effectiveness-number of transfer units
E-*XXXX*	Heat exchangers
HE	Heat exchanger
HFR	High Flux Reactor
IPCM	Implicit pressure correction method
K	Flow loss coefficient
LEU	Low-enriched uranium
MTR	Materials Testing Reactor
Necsa	South African Nuclear Energy Corporation
NEMA	National Electrical Manufacturers Association
NRU	National Research Universal
NPSH	Net Positive Suction Head
OWT	Outlet Water Temperature
PBMR	Pebble Bed Modular Reactor
P-*XXXX*	Pumps
P&ID	Piping and instrumentation diagram
RELAP	Reactor Excursion and Leak Analysis Program (Software)
RPM	Revolutions per minute
SS	Shell side of a shell-and-tube heat exchanger
T-*XXXX*	Ball catcher
TS	Tube side of a shell-and-tube heat exchanger
V-*XXXX*	Valves
X-*XXXX*	Chiller units
WCTPE	Wet Cooling Tower Performance Evaluation
Y-XL	Y- and basket strainers

Glossary

Term	Description
Atomise	The mechanical subdivision of a bulk liquid to produce small drops (3)
Centrifugal pump	Turbomachines employing centrifugal effects for increasing fluid pressure (5)
Chiller units	Two devices under alternate operation, that facilitate the successive exchange of heat between the air conditioning units to the internal refrigerant, from which the heat is exchanged to the secondary cooling system, which are all at different temperatures while keeping them from mixing with each other (6)
Computational fluid dynamics	The analysis of systems involving fluid flow, heat transfer and associated phenomena such as chemical reactions by means of computer-based simulation (1)
Counter-flow	Under the Wet Cooling Tower Performance Evaluation (WCTPE) transfer model software program, the counter-flow transfer model refers to the type of heat and mass transfer model, together with all their variables, required to solve the model. There are three mathematical models, each with their advantages, namely the Merkel model, Poppe model and the effectiveness-number of transfer units (E-NTU) method (7).
Degasifier	A device that removes contaminated gas from the condenser primary system. The condenser facilitates the exchange of heat between the two fluids, under which one of the fluids undergoes a phase change of the degasifier system and the secondary cooling system, which are at different temperatures, while keeping them from mixing with each other (6).

Draft options	Under the WCTPE software program, draft options refer to the options for the software to calculate the air flow rate if this data is not available (7)
Fan coil units	Multiple devices in parallel that facilitate the exchange of heat between the two fluids of the primary pump room and the secondary cooling system, which are at different temperatures, while keeping them from mixing with each other (6)
Flownex® designer	Flownex designer is a first-generation direct design and optimisation facility that has been developed and implemented into Flownex SE (37)
Heat fraction	In a turbomachine, the heat fraction is a fraction of the energy that does not directly contribute to increase in fluid pressure. This energy contributes to the increase in temperature of the fluid media and surroundings (8).
Induction motor	An induction motor is an alternating current electric machine that converts electrical energy into mechanical energy. It rotates slower than the line frequency in order to develop torque (9).
Loss coefficient	The adimensional difference in the total pressure between the ends of a straight pipe or respectively other pipe geometries (10)
Low-enriched uranium	Low-enriched uranium has a lower than 20% enrichment (2).
Net Positive Suction Head	The minimum suction head required for a pump to operate (3)
P&I diagram	A diagram that shows the interconnection of process equipment and the instrumentation used to control the process. In the process industry, a standard set of symbols is used to prepare drawings of processes (4).
Pool heat exchanger	A device that facilitates the exchange of heat between two fluids of the reactor pool and the secondary cooling

	system, which are at different temperatures, while keeping them from mixing with each other (6)
Primary system	The reactor primary system and the pool primary system, where water circulates to cool the associated components (19)
Psychrometric	Of or relating to the determination of physical and thermodynamic properties of gas-vapour mixtures (3)
Secondary water monitor	A monitoring system that measures for trace amounts of monitor radioactive substances in the secondary cooling system's water
Shell-and-tube HE	A shell-and-tube heat exchanger is a device that facilitates the exchange of heat between the two fluids, one flowing in a shell and the other fluid flowing in tubes axially with the shell, that are at different temperatures while keeping them from mixing with each other (6)
Secondary system	The secondary cooling system whereby the heat from the primary side is removed through a series of heat exchangers (19)
Solution control	Under the WCTPE software program, solution control refers to the various parameters under which the model must solve, such as the maximum number of allowed iterations, the convergence solution criteria, the relaxation values, which assist in preventing numerical instability, and the initial estimates for the program to initiate (7) (11)
Static temperature	The temperature that is measured moving with the fluid (14)
Synchronous	A synchronous motor is an AC motor electric machine that converts electrical energy to mechanical form and rotates in synchronism with the line frequency (9)
Total temperature	The temperature obtained by isentropically bringing the flow to rest (25). For incompressible flows, total

	temperature is equal to static temperature (14).
Transfer characteristics	Under the WCTPE software program, the transfer characteristics refers to the equations and physical values required to determine the energy transferred in each discreet area within the tower, such as the heat transfer coefficient of the spray zone, rain zone and the effect of the water quality and the type and arrangement of the cooling tower internals (7), (6).
Tube-cleaning system	A parallel, on-line tube-cleaning system pioneered by system Trapogge®. The system allows small foam rubber balls to circulate through the tubes of a tubed heat exchanger to reduce fouling and so increase the equipment life and efficiency (12).
Turbomachine	A device in which kinetic energy is transferred either to or from a continuously flowing fluid by the dynamic action of one or more moving blade rows (5)
Valve flow	The relationship between the percentage flow and the characteristic valve stroke (13)
Wafer check valve	Check (non-return) valves are installed in pipelines to allow flow in one direction only, which helps to protect equipment and processes. Wafer check valves are a variation designed to fit between a set of flanges (14).
WCTPE software	Software specifically designed for the performance prediction and evaluation of wet cooling towers

1. Introduction

1.1 Background

SAFARI-1 is a Materials Testing Reactor (MTR) tank-in-pool research reactor with a licensed operating thermal power of 20 MW, located at Pelindaba to the west of Pretoria, South Africa. The reactor is a major producer of medical and industrial isotopes for domestic and international consumption. The production of these isotopes are organised on a commercial and contractual basis. The reactor has been operational for approximately 47 years. Similar to other research reactors, it has been affected several factors during this time, including the following (15):

- Extreme changes in its utilisation profile
- Outdated or obsolete technology
- Aging components and personnel
- Political influences and a changing public
- Regulatory demands regarding safety and risk of operation

The SAFARI-1 reactor project was initiated in September 1960 and construction started in 1961. The reactor was commissioned in March 1965. Initially, the cooling capacity was installed for a reactor power of 6.67 MW and the reactor was operated at this capacity. During 1968, significant upgrades were made to the reactor's primary and secondary cooling systems, allowing the reactor's capacity to be increased to 20 MW (15).

In 1976, an embargo was placed on the supply of fuel to SAFARI-1. The operating power was reduced to 5 MW and the operating hours were greatly reduced (four days a week at a stage) in order to conserve fuel stocks while a local enrichment and fuel manufacturing capability was developed. In 1981, the first locally produced fuel assemblies became available and the reactor was operated for five days a week at 5 MW until 1993. In 1993, the focus of SAFARI-1 operations was shifted to commercial applications. The nominal power level was initially increased to 10 MW, with gradual more frequent operation at 20 MW for the development and implementation of commercial isotope production programmes (15).

1.2 Motivation

Currently, the SAFARI-1 reactor indirectly supplies radioisotopes to nearly 60 countries around the world through low-enriched uranium (LEU) fuel technology and is one of only five reactors in the world to produce Mo-99. As was seen with outages at Canada's National Research Universal (NRU) reactor (2009 to 2010) and the Netherlands' High Flux Reactor (HFR) (2008 to 2009), major disruptions in supply of Mo-99 resulted in many patients not having access to radio diagnostics treatment. The inability to keep radionuclide production constant has negatively affected multitudes of patients who rely on radionuclide and associated technologies for their treatments (16, 17).

Limiting the downtime of such facilities is crucial, not only to the economic benefit of the reactor operators, but also to the multitude of patients who rely on the radio diagnostic treatment and therapy.

Currently, SAFARI-1 is scheduled to be retired by the year 2020, with a new reactor that will focus solely on the production of radioisotopes planned for the Pelindaba site. Until such time as the new reactor has been completed and SAFARI-1 potentially undergoing refurbishment, the responsibility of keeping it in optimal running condition rests on the SAFARI-1 operational staff (17).

Within the SAFARI-1 reactor system, the secondary cooling circuit requires engineering characterisation, which removes the heat from the primary cooling circuit. The cooling system's capacity and performance is currently questioned. It is not sure that the operational performance is optimal. If there is a dissonance between the designed capacity and the actual capacity, it could point to an array of potential causes, which, could potentially affect the availability of the system as a whole in varying degrees.

Setting up a thermohydraulic model that accurately represents the secondary cooling system of SAFARI-1 could thus not only identify problems and/or inefficiencies within the current system, but can also be used to evaluate potential future changes or introduce adjustments to the system in order to achieve optimal performance.

1.3 Previous investigations

The initial design of the cooling circuit was done by mainly “manual” calculations. This method, although partially verified by physical measurements after completion, does not capture the synthesis of a complex interdependent system such as the secondary cooling system.

In 1964, prior to its official commissioning, an internal effort was made to form a database to capture all the elements within the circuit. This database was based on a card system that contained all relevant data of the different elements in the cooling system and referred to all additional information pertaining to it, but this database has unfortunately been lost.

Recently, after a virtual absence of data on the secondary cooling system, an internal effort has begun to characterise the secondary circuit, and a simplistic model has been constructed using the same software that was employed for this study.

Currently, though, there is no accurate integrated model that captures the complex interdependence of the different parts of the system.

1.4 Objectives

Setting up a thermohydraulic model, using the software Flownex®, that represents the current configuration of SAFARI-1’s secondary cooling system entails the following:

- The model should contain all the systems, structures and components of the current cooling system.
- The requirement/function of each system, structure and component within the system shall be listed.
- The design and performance data of the systems, structures and components are to be used to construct the model. Where data is not readily available, alternative data could be used, but will need to be motivated before it is incorporated into the model.
- All assumptions for the model should be listed.
- The model shall be verified by comparing the theoretical results to the existing

hardware performance data.

- This model should be used to evaluate future improvements to the secondary cooling system.
- This project should help students and other future users of this model to understand the secondary cooling system.
- The construction of this model will afford the author the opportunity to demonstrate his understanding of the theory by modelling the entire secondary cooling system.
- It should allow the student to make proper assumptions and verify the theoretical model's results against the physical hardware performance data of the secondary cooling system.
- Additional test data might be required to verify the model for correctness.
- The project provides the student the opportunity to use simulation software for the analysis of a typical cooling system.
- Additionally, this project could be used to demonstrate the potential integration of this model with other computational fluid dynamics (CFD) simulation packages.

1.5 Limitations of the study

Currently, there are two major limitations to the study: the lack of detailed data on components in the system and the sensitive nature of the information due to the associated commercial rights and confidential classification of nuclear facilities.

1.5.1 Insufficient data

Due to the system's age, a lot of the data is impossible to retrieve from the original manufacturers, as many of the companies that supplied certain critical components do not exist anymore. Therefore, alternative data was generated wherever original data was inaccessible or non-existent. Recorded data points of process parameters at specific locations in the secondary cooling system are also limited as the secondary cooling system does not necessitate the logging of data as done for the primary loop.

1.5.2 Sensitive and proprietary information

The information employed in this study is of a sensitive nature, as it is regarded by the owner as being commercial assets of significant value. Therefore, certain limitations on access and provision of information are put in place. This involves not reproducing or displaying any information that is not essential to achieve the required result and limiting access to this information. It was therefore agreed to limit the information in the main body of work by only referring to the information required to explain key concepts and verify results. The constructed model (Appendix I), all the model inputs (Appendix II) and model results (Appendix III) that are not essential to understanding the main body of work, but are considered significant to the owner, are appended as such and are considered proprietary information. To access this information, written permission is required from the South African Nuclear Energy Corporation (Necsa).

2. Literature

The secondary cooling system, as the name suggests, is the cooling system that finally transfers the heat from the SAFARI-1 reactor to the main heat sink, which is the cooling tower. The two systems work in series, and the primary cooling loop is in direct contact with the reactor core where energy (heat) is taken up. This energy is a by-product of nuclear fission and decay of fission products, which is of no particular use in the case of a non-power reactor. Demineralised water is forced through the core by pumps, where energy is then transferred to this medium (based on the principle of the second law of thermodynamics) and is forced through heat exchangers to transfer the energy to the secondary side (based on the principle of the second law of thermodynamics) (18).

The secondary cooling system works on a similar principle to the primary loop in which the heat transfer medium is water. This water is once again pumped through a series of pipes and ancillary systems to remove the energy (heat) from the heat exchangers to the cooling towers that serve all subsystems, which in turn release the energy (heat) into the atmosphere. The ancillary systems referred to above include, but are not limited to, the pool heat exchanger, the fan coil units, the chiller units, the tube-cleaning system, the degasifier condenser and the secondary water monitor.

All the systems that form part of the secondary cooling system will be briefly discussed in this chapter, together with the methods of analysing such systems and the tools for completing such an analysis (19).

The methodology of temperature control along with a justification of the physical layout of the model is attached in Appendix IV and Appendix V respectively, as this information is not central to understanding the main purpose of this document.

2.1 The secondary cooling subsystems

The following is a brief discussion of the subsystems that constitute the secondary cooling system and the parts and terms that might be considered foreign to the uninformed reader.

2.1.1 Cooling tower subsystem and secondary water monitor

Traditionally, cooling towers are heat exchangers that utilise a mixed flow of two fluids in different phases. It allows heated water to transfer its energy, via the second law of thermodynamics, to the ambient air. To increase the heat transfer, the water is atomised, which allows a greater heat transfer area between the droplets and the surrounding air. The cooling towers employ fans (labelled iv in **Figure 1**) to force the air through the tower in the opposite direction of the water droplet movement. This increases the amount of cooler air relative to the water droplets that is available for effective heat transfer.

The cooling towers referred to in this text are defined as two-cell, mechanical draft, counter-flow wet cooling towers (7). This implies that there are two identical cells per tower, which employ fans in each cell to create forced relative movement between the water droplets and the ambient air. Due to the nature of energy transfer, small amounts of water evaporate into the atmosphere. To counter this effect, there is a feed water system that keeps the water levels within the cooling tower basins relatively constant. Since this process is a local process (within the confines of the cooling tower) and only the total energy transfer within the cooling towers is considered, the process of water makeup and evaporation is considered to be equal and opposite. Therefore, it is superfluous to the model (19).

The secondary water monitor is a monitoring system that measures trace amounts of radioactive substances within the secondary cooling system. This is a safety precaution in the event that there is a significant breach and/or leak from the primary side into the secondary cooling system. The secondary water monitor is a passive system, which relies on the main system pressure to force the water sample through the monitor. This process adds no energy and due to the minute flow volumes encountered in this system, it was deemed statistically insignificant when considering the overall system. It was therefore not included in the study.

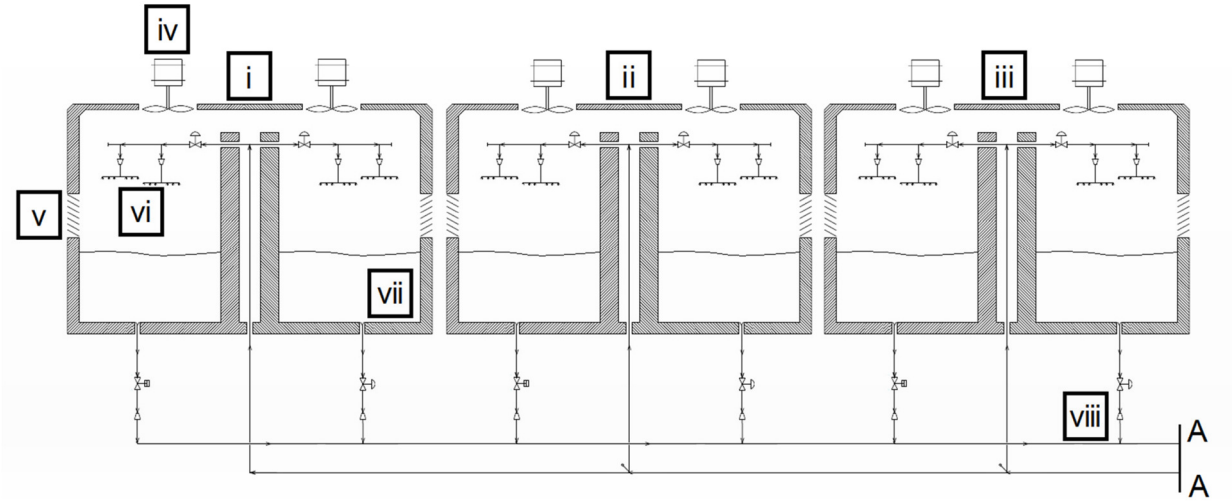

Figure 1: Cooling tower subsystem

The following elements of **Figure 1** are described for clarity:

A-A. Boundary interface plane between cooling tower subsystem and secondary water monitor, and the secondary side of the primary heat exchanger and tube-cleaning subsystems

i. East two-cell, mechanical draft, counter-flow wet cooling tower

ii. Centre two-cell, mechanical draft, counter-flow wet cooling tower

iii. West two-cell, mechanical draft, counter-flow wet cooling tower

iv. Cooling tower fan unit

v. Air inlet

vi. Spray nozzles

vii. Cooling tower basin

viii. Reducer (as typically found throughout the system)

2.1.2 Primary heat exchanger and tube-cleaning subsystems

The primary heat exchanger subsystem removes heat from the core of the reactor. This is achieved through the combined effects of the elements mentioned in the schematic diagram of the subsystem in **Figure 2**. It can be seen from **Figure 2** that the secondary pumps draw water from the cooling towers. In turn, these pumps feed the primary heat exchangers. The water then flows back into the cooling towers. Additionally, a tube-cleaning system, pioneered by Trapogge®, circulates small foam rubber balls through the tubes of the primary heat exchangers to avoid unwanted fouling deposits (12). A simplified view of the subsystem is depicted in **Figure 2** (19).

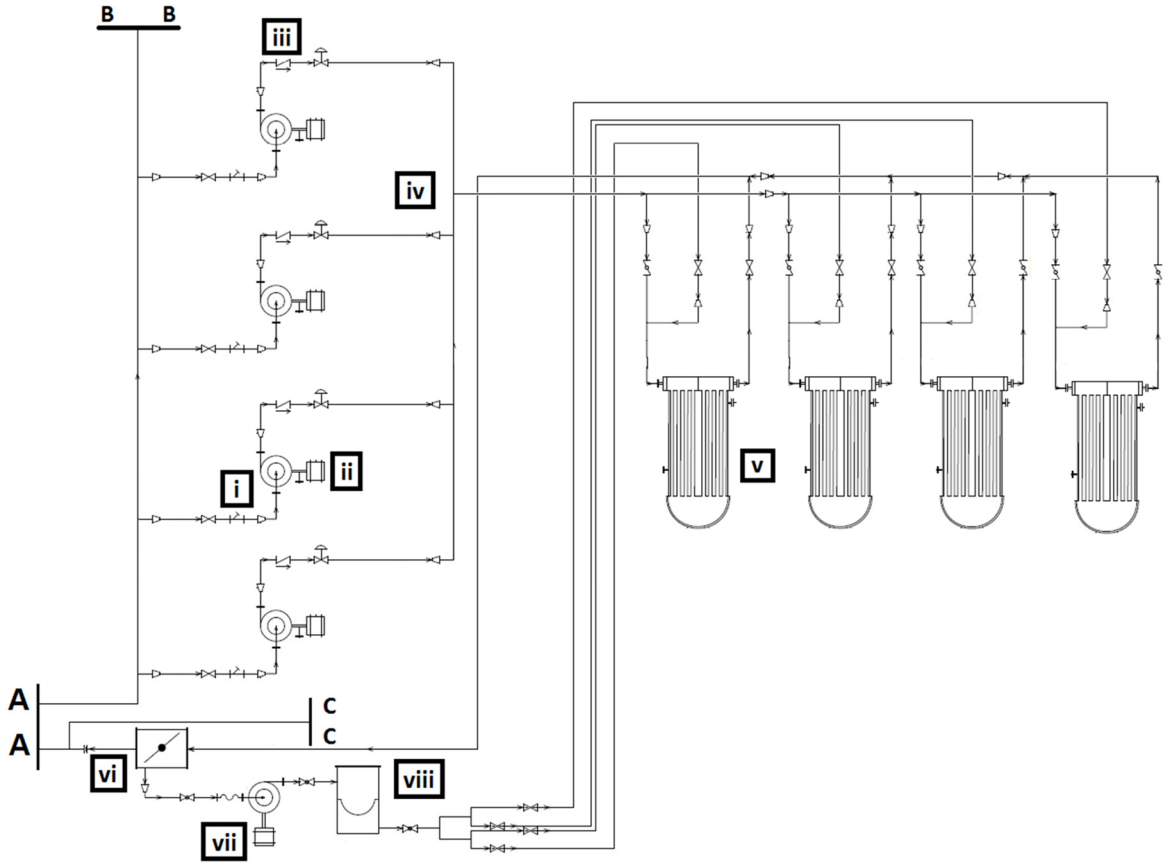

Figure 2: Primary heat exchanger and tube-cleaning subsystems

The following elements of **Figure 2** are described for clarity:

A-A. Boundary interface plane between the cooling tower subsystem and secondary water monitor, and the primary heat exchanger and tube-cleaning subsystems

B-B. Boundary interface plane between the inlet of the pool heat exchanger, degasifier condenser subsystems, secondary water monitor, primary heat exchanger and tube-cleaning subsystems. The pool heat exchanger subsystem is described in 2.1.3

C-C. Boundary interface plane between the outlet of the pool heat exchanger, degasifier condenser subsystems, secondary water monitor, primary heat exchanger and tube-cleaning subsystems

i. Basket strainers are high-flow filters that trap unwanted debris that might enter the system at the cooling tower. This limits potential damage to downstream elements that are sensitive to debris.
ii. Secondary cooling pumps. These pumps are typical industrial centrifugal pumps.
iii. The check valves found in the system are wafer check valves.
iv. The Y-joint found at this point is a non-standard joint and can be described as two angled inlets combining into a vertical third leg.
v. The heat exchangers referred to are typical shell-and-tube heat exchangers with the secondary cooling fluid flowing on the tube side.
vi. The ball strainer at this point is a separating screen employed to remove the sponge rubber balls from the main system to facilitate the effective re-introduction into the heat exchangers.
vii. The ball recirculating pump is a typical centrifugal pump.
viii. The ball catcher is a high-flow sieve where the foam balls (if so desired) can be isolated for inspection and replacement.

2.1.3 Pool heat exchanger and degasifier condenser subsystems

The pool heat exchanger subsystem removes heat from the pool water in which the reactor vessel and spent fuel is kept. The heat from the reactor vessel can be described as excess heat that is not removed by the primary heat exchanger subsystem. A relatively small amount of heat is generated by the spent fuel through

decay. The system, together with the primary heat exchanger subsystem, ties in with the cooling towers from where the water is pumped through heat exchangers, and again joins the main line into the cooling towers between interface C-C and A-A, as seen in **Figure 2**. An inlet from the degasifier condenser system ties in between the pool heat exchanger and the place where the line ties in with the main inlet line to the cooling towers. This is recognised as a system source and effectively creates an open loop system. It should be noted that the degasifier condenser system would greatly complicate an analysis of the system. It has therefore been omitted for the purpose of this study due to the negligible thermohydraulic effect on the system as a whole.

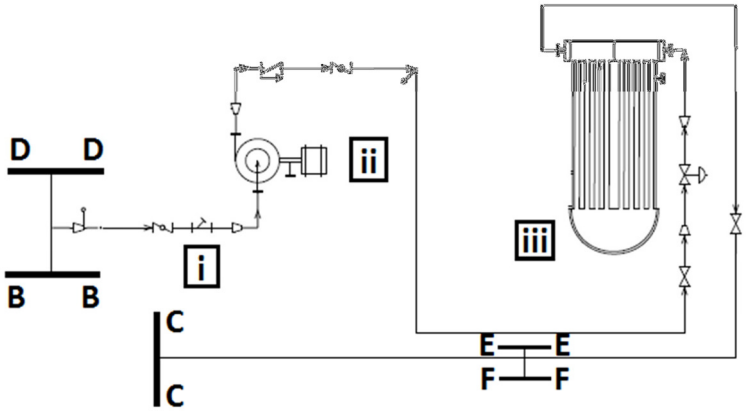

Figure 3: Pool heat exchanger subsystem

The following elements of **Figure 3** are described for clarity:

B-B. Boundary interface plane between the inlet of the pool heat exchanger, degasifier condenser subsystems, secondary water monitor, primary heat exchanger and tube-cleaning subsystems

C-C. Boundary interface plane between the outlet of the pool heat exchanger, degasifier condenser subsystems, secondary water monitor, primary heat exchanger and tube-cleaning subsystems

D-D. Boundary interface plane between the pool heat exchanger, degasifier condenser subsystems, chiller units and fan coil unit subsystems

E-E. Boundary interface plane between the pool heat exchanger, degasifier condenser subsystems, chiller units and fan coil unit subsystems

F-F. Boundary interface plane between the pool heat exchanger, degasifier condenser subsystems, chiller units and fan coil unit subsystems

i. Y-strainers are low-flow filters that trap unwanted debris that might enter into the system at the cooling tower. This limits potential damage to elements downstream from the strainer that could be sensitive to debris.

ii. The pump referred to is a typical industrial-type centrifugal pump.
iii. The pool heat exchanger is a typical shell-and-tube heat exchanger with the secondary cooling fluid flowing through the tube side.

2.1.4 Chiller and fan coil unit subsystems

The chiller units employed indirectly cool air in specific parts of the reactor building. The chillers work on the principle of the vapour compression cycle to cool water that is utilised through various heat exchangers at specific points in the buildings. The working fluid of the abovementioned process should not be confused with the working fluid of the secondary system, as these are two separate systems. The secondary cooling system comes into play as these chillers are water cooled and so rely on the secondary cooling system to fulfil this role. It therefore removes energy from the chiller units produced in the vapour compression cycle. The chillers are employed on an alternate basis, with one on stand-by. The fan coil units are also employed to cool specific rooms (more specifically, the primary pump rooms). However, it is a direct cooling system with a line of the secondary cooling system coupled to heat exchangers to remove the heat generated within the pump rooms. There is very limited data available on these heat exchangers, but since the fluid volumes through them and the associated energy is relatively small, the assumptions made were deemed sufficient to analyse the system.

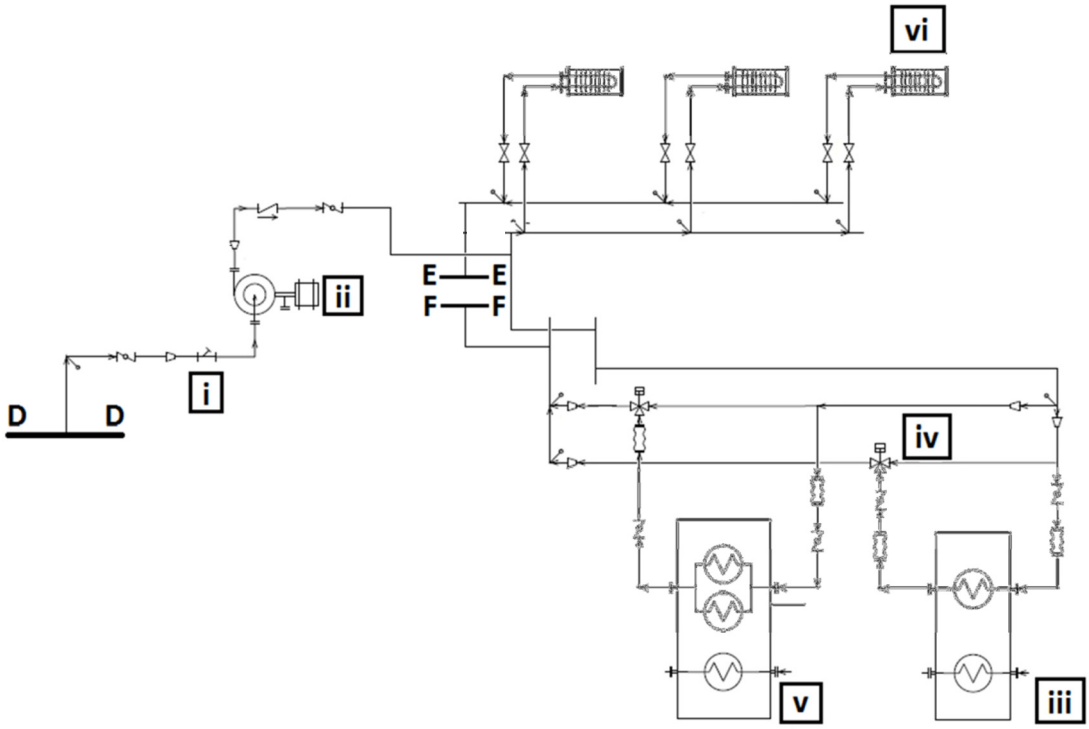

Figure 4: Pool heat exchanger subsystem

The following elements of **Figure 4** are described for clarity:

i. The Y-strainers found here are similar to the unit mentioned under the pool heat exchanger and degasifier condenser subsystem, but is physically smaller.
ii. The pump referred to is a typical industrial-type centrifugal pump.
iii. The chiller (Daikin) is a water-cooled reciprocating liquid chiller.
iv. A three-way valve allows flow through two of the possible three legs. This allows for bypass of either of the chiller units.
v. The chiller (Carrier) is a water-cooled reciprocating liquid chiller
vi. Fan coil units are two-pipe (one supply and one return pipe) fan coil units. These coils are located in the ducts through which air flows to cool specific areas or rooms in the building. The exact inner geometry and construction is unknown, but it can be considered in simple terms as a cross-flow heat exchanger.

3. Method of analysis

3.1 Methods of analysis

The analysis of thermohydraulic systems can be performed using several different methods. The methods considered relevant to this study are first principles, analytical analysis, CFD and one-dimensional solvers (20, 21). These methods all have their strengths and weaknesses, depending on the application and scale of the investigation.

3.1.1 First principles

This is the most basic of the methods that can be employed, but this process is extremely labour intensive when one considers the number of integral parts in the system and the various conditions under which they operate. Due to the nature of the fluid, applying equations, such as the Navier-Stokes equation, to the complex geometries found in the system is virtually impossible as only “simple” geometries have been solved (1). The amount of variables that will have to be considered and the assumptions that will have to be made to account for the lack of available information would render the model ineffective.

3.1.2 Analytical analysis

Analytical analysis stems from experimental work where formulae were developed for systems where the behaviour could effectively be described or represented by specific formulae. This is a progressive process where the accuracy of the given formulae is determined by the accuracy of the equipment used in the said experiments. This, in conjunction with the vast amount of varied, characterisable systems, leaves one with only basic geometries with sometimes large margins of error. This method still merits its widespread use, as specific geometries have undergone exhaustive testing, having very small margins of error and effectively eliminate the need for in-depth knowledge of certain systems to effectively predict system behaviour. These formulae are also easily integrated into software packages, and are therefore an invaluable tool in the engineering field (1).

3.1.3 Computational fluid dynamics

CFD is the analysis of systems involving fluid flow, heat transfer and associated phenomena, such as chemical reactions by means of computer-based simulations (1). For an accurate model to be generated, the discretisation has to be on such a scale that it fully incorporates the effects of complex geometries as they would be found in typical systems. This discretisation process allows for the application of the conservation laws that govern the solution. Due to the system's large size as a whole and the detail required to accurately model detailed phenomena within individual components (the strength of CFD), the scale of the required mesh and the number of cells necessary to accurately model multiple components in series as a system, would far exceed the computational capabilities of any current hardware available for this study. CFD excels in the analysis of smaller individual components (computing power permitting), and one can easily determine the flow, heat transfer and other phenomena within the system components.

3.1.4 One-dimensional solvers

One-dimensional solvers work on the same basis as CFD packages, but apply a network approach to the individual elements within the system. Conservation of mass and energy are applied to the individual nodes that connect elements, and the momentum equations are applied to the element, all based on average values (22). This, together with analytical formulae that are pre-programmed into the software to account for the typical behaviour of such an element, i.e. a pipe element, allows for greatly reduced computational times and power. This differs from CFD where individual elements are modelled in sufficient detail to describe the physical geometry, the relative arrangement of the cells representing the geometry and the properties of the fluid being considered.

3.1.5 Conclusion

Based on an analysis of the above methods, a one-dimensional solver was deemed the most appropriate for the system analysis. For individual component analysis, a combination of analytical, CFD and one-dimensional methods was deemed necessary, depending on the geometry, the unknown variables, computational time and computing constraints.

3.2 Employed Software

3.2.1 One-dimensional solver: Flownex®

Flownex® is a one-dimensional thermal fluid design and analysis tool that is used extensively in practice for system and subsystem level simulations. The reason for choosing Flownex® as the governing solver for this study is its capabilities for constraint design, optimisation and sensitivity analysis of component or system parameters (8). Flownex® is also extensively validated and verified to stringent local and international standards. What sets Flownex® apart from other commercial codes is its ability to also model the effect of nuclear heat generation in a system. The current study does not include the primary system, which is affected by nuclear heating in the core. However, if such a model is required in the future, an extensive model that includes both systems can easily be generated (23, 8).

Flownex® is an evolution of the original code called Flownet®, which was based on the Hardy-Cross method to solve air and water distribution networks on mines. The code evolved and included developments such as the implicit pressure correction method (IPCM) algorithm. Further developments included the ability to deal with aircraft engine combustion systems, dynamic simulations of networks with time- dependent flows, code extensions to simulate the Pebble Bed Modular Reactor (PBMR) and the implementation of gas mixtures and conduction elements. Flownex® was subsequently developed from Flownet® as an object-oriented version. Since then, advances in the program include the following (23, 8):

- Implementation of rotating components and subnetworks
- Development of the homogeneous two-phase modelling capability
- Combustion modelling, momentum addition, radial pressure gradient

- Equation element, API, parametric layers, pipe schedules
- Release of new Flownex® simulation environment with control and electric modules and Excel integration
- Flownex® simulation environment, in-condensable, ASPEN fluid integration
- Slurry flows, detailed combustion, computer-aided design (CAD) and other importers
- Expanded two-phase flow, expanded heat transfer, trace elements and coupling to the nuclear code RELAP that analyses nuclear reactor core transients

All of the above stemmed from the industry-specific need to address complex thermo-flow systems (23, 8).

Flownex® provides the ability to model the complete integrated system, which allows engineers to quickly and accurately size components, do flow balancing and test different control methodologies in real time. Standard components with different levels of complexity are linked together in an arbitrary way to build any flow system. This is facilitated through an easy-to-use graphical user interface and the results are presented in a powerful graphical output (23, 8).

This “freedom” to arrange arbitrary links and connections acts as an ideal tool to simulate complex thermo-fluid systems as encountered in this study (23, 8).

Basic modelling principles

Flownex® solves the partial differential equations of mass, momentum and energy conservation over unstructured networks to determine the mass flow, temperature and pressure of the individual elements and nodes, where different elements couple. Nodes are endpoints to elements and together they form a network. Additional elements can be added to the nodes (a junction point) to create a large, unstructured network. An element is typically a component over which a pressure drop occurs, where the laws of conservation of momentum are applied and nodes act as the endpoints where the laws of conservation of energy and mass are applied.

An in-depth discussion of the general governing equations and the solver implemented by Flownex® is deemed unnecessary for the purpose of this study and it is therefore not discussed. If the reader wishes to do so, he or she can consult the Flownex® Library

Manual (8).

Model

The simulation performed is of a physical network representing the secondary cooling system of the SAFARI-1 research reactor. A simplified representation of the physical set-up of the system can be seen in **Figure 5**. The generated model, as seen in Appendix I, simulates the physical set-up as accurately as possible with current information and capabilities.

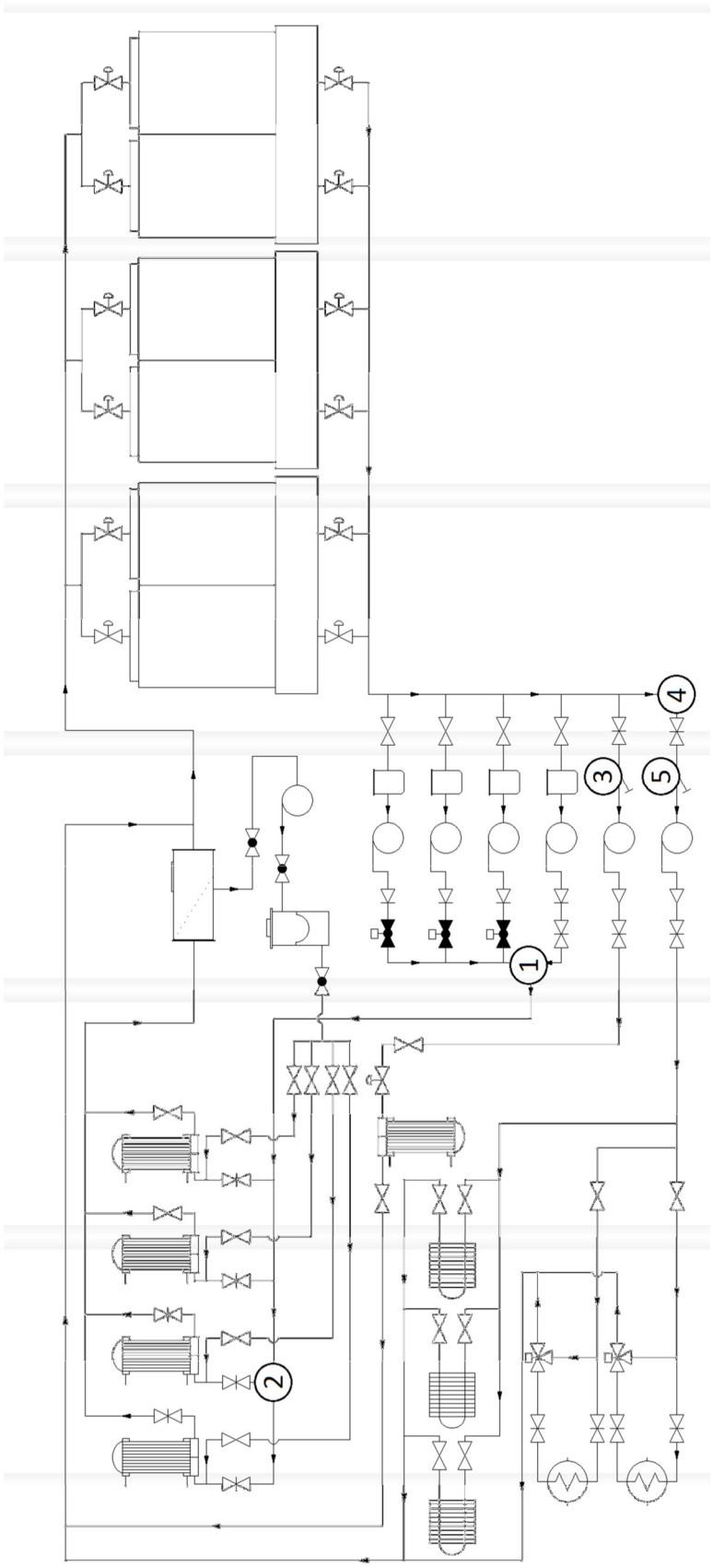

Figure 5: Schematic of the secondary cooling system

The employed simulation is a steady-state solution. Therefore, certain dynamic phenomena that could affect the process from within the system are not considered. These phenomena are typically valve opening and closing speeds, which are the effects of sudden transients within the secondary system that occur regularly during steady-state operation. This should not affect the overall results significantly, as there is a sufficient level of damping due to the large volume and accompanying inertia of coolant in both primary and secondary cooling systems.

The analysis will be of a pseudo-transient nature as boundary conditions can be adjusted for different scenarios that can be found within the system. The availability of certain components can also be changed to simulate emergency or abnormal scenarios.

It is assumed that the cycle only operates within the single-phase flow region. This assumption is slightly erroneous, as significant evaporation is experienced within the cooling towers. The water makeup line confirms this statement. This assumption is deemed to be beyond the scope of this study. Not having to consider the evaporation effect allows for the assumption of a closed loop system and the steady-state analysis is greatly simplified by reducing the number of variables within the system. As there are also no large changes in density or high Mach numbers expected in the system, the working fluid can be assumed to be incompressible (24).

Components

To familiarise the reader with the basic principles of the modelling of components, the example for the basic pipe element is employed. The Darcy-Weisbach equation can be employed in this element where pressure drop over the length of a horizontal pipe is described as (24, 8):

$$\Delta \boldsymbol{p} = \boldsymbol{f} \frac{\boldsymbol{L}}{\boldsymbol{d}} \frac{\boldsymbol{V^2}}{\boldsymbol{2}} \boldsymbol{\rho} \qquad [1]$$

Where:

Δp	=	Pressure drop
f	=	Darcy friction factor
L	=	Pipe length
d	=	Hydraulic diameter
V	=	Mean flow velocity*
g	=	Gravitational acceleration
ρ	=	Density

*unless a location is specified

To allow the solver to discern between a pressure rise or pressure drop, depending on a positive or negative relative velocity over the element, the convention of writing the velocity term changes the formula to the following:

$$\Delta \boldsymbol{p} = \boldsymbol{f}\frac{\boldsymbol{L}}{\boldsymbol{d}}\frac{|\boldsymbol{V}|\boldsymbol{V}}{\boldsymbol{2}}\boldsymbol{\rho} \quad [2]$$

To account for changes in elevation and the inlet and outlet loss coefficients, the following terms are added (24, 8). It should be noted that Equation 3 shows the entire formula and not only the additions due to elevation and loss coefficients.

$$\Delta \boldsymbol{p} = \boldsymbol{f}\frac{\boldsymbol{L}}{\boldsymbol{d}}\frac{|\boldsymbol{V}|\boldsymbol{V}}{\boldsymbol{2g}} + \boldsymbol{\rho g}\Delta \boldsymbol{z} + \boldsymbol{K_i}\frac{\boldsymbol{1}}{\boldsymbol{2}}\boldsymbol{\rho}|\boldsymbol{V_i}|\boldsymbol{V_i} + \boldsymbol{K_e}\frac{\boldsymbol{1}}{\boldsymbol{2}}\boldsymbol{\rho}|\boldsymbol{V_e}|\boldsymbol{V_e} \quad [3]$$

Where additionally:

K	=	Loss coefficient
Δz	=	The relative change in (height)
i	=	Inlet
e	=	Outlet

This is the approach employed to account for expected pressure variations within a standard pipe element, as found in Flownex®.

The basic principle for standard elements, such as bends or elbows, is integrated as

loss coefficients, as determined by models of Idelchik, Miller and Crane (8), which rely on predetermined loss coefficients. For the detailed equations employed within the Flownex® software for all other elements, the reader is referred to the Flownex Library Manual (8).

3.2.2 Computational fluid dynamics: STAR CCM+

Typical CFD analysis programs make use of three different numerical solution techniques: finite difference, finite element and spectral methods. The method employed by Star CCM+ is the finite volume method. This is a special finite difference formulation that is central to the most well-established CFD codes (1).

STAR CCM+ is a modern engineering simulation tool that provides a suite of related components integrated within one software environment. These components include the following:

- 3D-CAD modeller
- CAD embedding
- Surface preparation tools
- Automatic meshing technology
- Physics modelling
- Turbulence modelling
- Post-processing
- CAE integration

STAR CCM+ is based on object-oriented programming technology and it is built using a client-server architecture. It is specifically designed to handle large models quickly and efficiently via a unique client-server architecture that seamlessly meshes and simultaneously solves pre- and post-processes over multiple computing resources without requiring additional effort from the user. STAR CCM+ recently became the first commercial CFD package to mesh and solve a problem with over one billion cells. The object-oriented nature of the code can be seen in the user interface.

An object tree is provided for each live simulation and contains object representations of all the data associated with the simulation. In the program, one can see the simulation objects associated with the fluid region and the various boundaries that have been defined for that region (25).

3.2.3 Analytical analysis: Wet Cooling Tower Performance Evaluation

Wet Cooling Tower Performance Evaluation (WCTPE) is a computer software program that was developed for use in the thermal design, analysis and performance prediction of wet cooling towers. The program allows for the analysis of the thermal performance of various wet cooling tower arrangements, such as natural draft counter-flow cooling towers, mechanical draft counter-flow cooling towers and cross-flow cooling towers (26, 27).

Basic modelling principles

WCTPE software caters for counter-flow forced draft cooling towers, as found at SAFARI-1. The solver is essentially a one-dimensional program, but it accounts for the three-dimensionality of cooling towers through semi-empirical equations, especially in the loss and transfer coefficients in the rain zone (26). To allow this one-dimensional approach, certain assumptions and simplifications have to be made. The following are assumed:

- Steady-state conditions are present with no wind blowing.
- Thermal loads, such as makeup water additions, pump head gain and net heat exchange with ambient surroundings, are negligible. The addition of pump heat input is accounted for as an input variable, as there is no pump within the confines of the control volume.
- Uniform air and water flow rates exist over the tower's cross-sectional area.
- The thermodynamic properties of the water and air vary only in a vertical axis, and remain constant through any horizontal plane (7).

The variable inputs not constrained within the program are too numerous and fall outside the scope of discussion for this thesis, but macroscopically, the input variables are the following (7):

- Ambient conditions
- The solution control and draft options
- The transfer characteristics
- The counter-flow transfer model settings
- Cooling tower dimensions and operating conditions
- Loss coefficients
- Fan specification

3.2.4 Howden cooling fans selection program (CF-P20 V6.07)

The cooling fan selection program is a comprehensive linear selection program, which accesses the comprehensive database of the Howden cooling fans company. This program, as a function of varying inputs for fans, generates relative data such as fan static pressure and fan shaft power.

Inputs

The program makes use of a full spectrum of information to determine the specific fan configuration. Once again, the variable inputs not constrained within the program are too numerous and fall outside the scope of discussion for this thesis, but in general terms, the input variables are the following (28):

- Restrictions in terms of minimum pressure margins and static efficiencies, and maximum fan power consumption
- Duty point
- Installation type, inlet shape, diffusor design and fan mounting orientation
- Obstacles at inlet and outlet side
- Fan diameter ranges and fan speeds

3.3 Statistical methods

When converting actual data into a usable format for the relevant software, difficulties arise, as there is a set formula to which the pressure drop relation has to subscribe to. The formula employed by Flownex® for pressure drop is a general empirical relationship (8) of the following form:

$$\Delta \boldsymbol{p_0} = \boldsymbol{C_k \rho^{\beta} Q^{\alpha}} \quad [4]$$

Where:

Δp_0	=	Pressure drop
C_k	=	Pressure drop constant
ρ	=	Mean density (based on the mean static pressure and temperature)
β	=	Pressure drop constant (related to density)
Q	=	Volume flow rate [m^3/s]
α	=	Pressure drop constant (related flow geometry)

To determine a trend in data, good practice is a minimum amount of three data points. In principle, this should capture the nature of the pressure loss curve over varying input data.

Difficulty was encountered when solving three simultaneous equations with only two variables, as seen below. A method of converting real-world data into a usable format prompted the use of a statistical method where a standard deviation was employed to achieve a “best fit” solution.

For the given model, the solution of $\beta = 1$ was assumed to be accurate, as there is no expected phase change in the system due to the pressures and temperature range encountered.

Running a simulation for a specific flow rate (Q) yields a pressure differential (Δp_0). Repeating the process at least twice at different flow rates yields different corresponding pressure differentials for the specific geometry.
An initial value of α is then set at the numerical value of 2 (this is generally accepted as

a good starting point). The equations for the separate flow rates and associated pressure drops are then used to calculate the values of the other constant (C_k). If the value of the guessed constant is erroneous, the corresponding values attained for C_k will not be a single numerical value. The standard deviation is then calculated for the acquired values of C_k. The constant (a) is then varied until the standard deviation is at a minimum. At this point, the average of the minimum of three attained values of C_k and the corresponding value of α is taken to be the final and most accurate representation of the constants.

A simple example of where this method is employed on a Y-strainer can be seen in Appendix VI.

3.4 Conclusion and summary of analysis methods

All the subsystems that form part of the secondary cooling system were discussed in this chapter. Foreign and uncommon terms and equipment were emphasised. The methods and the level at which they would be employed to ensure addressing all the aspects of the various systems and subsystems were briefly discussed. The tools for completing the various analyses were briefly introduced and described. The employed software makes use of the abovementioned methods and their particular functions were briefly discussed to ensure the reader has a firm grasp of the limitations and advantages of employing the listed software. Statistical methods employed were also described to address some of the variables that do not allow for ideal mathematical solutions.

4. Results

This chapter depicts the organisational hierarchy of the secondary cooling system. The most basic level is the analysis of the structures and components that make up the various subsections. The next level is the analysis of various integrated subsections. Finally, all the subsections are combined in the synthesis subsection, giving the result for the system as a whole.

4.1 Structures and components

To effectively model the secondary cooling system, the systems have to be dissected into their individual structures and components. To support these models of the relevant structures and components, sufficient data has to be available to accurately model the structures and components that make up the model. The following section describes the methods employed, and the results of such investigation to process incoherent data into a format that supports meaningful analysis in specific structures and components of which the data is not readily available.

4.1.1 Procedural analysis of structures and components

An in-depth discussion of all the various structures and components within the secondary cooling system is considered unnecessary, as most of the models employed are standard within the Flownex® package and have been qualified to stringent codes that agree with best engineering practices. For an in-depth analysis of each of the components, the reader is referred to the Flownex Library Manual (8).

What follows below is a more detailed discussion of specific parts where it was deemed necessary, where alternative methods were employed or considered, or where assumptions had to be made.

Valves

DESIGNATION: V-0601, V-0609, V-0616, V-0621, V-0628, V-0675, GV-0000, GV- 0001, GV-0011, GV-0015, GV-0017, GV-0184, GV-0019, GV-0002, GV-0212, GV-0213, GV-0214, GV-0215, GV-0216, GV-0217, GV-0218, GV-0219, GV-0220, GV-0221, GV-0222, GV-0223, GV-0248, GV-0003, GV-0030, GV-0336, GV-0356, GV-0367, GV-0041, GV-0410, GV-0422, GV-0430 GV-0045, GV-0048, GV-0049, GV-0053, GV-0054, GV-0055, GV-0056, GV-0571, GV-0066, GV-0071, TCV-0054, TV-0001, TV-0002, TV-0003, TV-0004, TV-0005, TV-0006, TV-0007, TV-0008, TV-0009, TV-0010, TV-0011, V-0269, V-0602, V-0604, V-0605, V-0606, V-0607, V-0612, V-0614, V-0622, V-0624, V-0627, V-0630, V-0632, V-0634, V-0635, V-0636, V-0640, V-0643, V-0647, V-0648, V-0649, V-0650, V-0677, V-0678, V-0679, V-0680, V-0681, V-0682, V-0603, V-0608, V-0610, V-0615, V-0617, V-0623, V-0625, V-0626, V-0651, V-0652, V-0674, V-0676, V-0683, V-0684, V-0687, V-0688

Due to the age of the system and the general lack of information on the parts in use, assumptions had to be made that could negatively influence the accuracy of the model when compared to the actual design. As there is insufficient data with regard to the valves in the system, the standard data with regard to loss coefficients was based on the data in the Flownex® database. The data is considered satisfactory, even though the author is aware that valve design has evolved to reduce certain losses over the years. A more accurate model would require expensive and timely testing.

The valve flow characteristic is assumed to be linear. This assumption is not based on any available data, but is considered irrelevant, as most of the valves (with the exception of certain control valves) are either in the fully open or closed position.

Basket strainer

Designation: Y-0601, Y-0604, Y-0605, Y-0606 (i in **Figure 2**)

There was no specific data relevant to the basket strainers apart from the diameter of the inlet and outlet nozzles of the strainers. External data was obtained with regard to the basket strainers of similar design and dimensions and it was deemed sufficient for an initial solution. The pressure loss data had to be incorporated into the Flownex® model into a custom loss element. This element allows the user to force specific pressure loss characteristics through the general empirical relationship of Equation 4.

Once again, it is assumed that there is no phase change in the coolant, and therefore, the only unknowns are the constants C_k and α. Data from the Sure Flow Equipment Inc. (29) was employed to set up three equations that could once again be solved, as mentioned earlier in Section 3.3. The results for the constants of the basket strainer can be found in **Table 1**.

Table 1: Sure Flow basket strainer empirical pressure loss constants

Pressure loss constants	Value
C_k	87.68
α	2.11

The assumption that the basket strainers installed within the secondary cooling system have similar pressure drop characteristics to that which is typically supplied by Sure Flow Equipment Inc. was found to be incorrect. This result was expected, as flow strainer design has evolved significantly since the advent of CFD design.

The interior dimensions of the currently employed basket strainers were not available to determine the required characteristics through CFD analysis. The type of flow curve, which is defined in the general empirical formula as a, was employed from the Sure Flow strainers, as it is assumed that the characteristic flow should be relatively the same due to shared design principles. The effective pressure drop would therefore be determined by varying the value of C_k to allow for adequate pressure drop over known intervals within the system.

The achieved value for the empirical pressure loss data was determined as in **Table 2**.

Table 2: Y-0601, Y-0604, Y0605, Y-0606 basket strainer empirical pressure loss constants

Pressure loss constants	Value
C_k	640
α	2.11

Reactor secondary water pump

Designation: P-0601, P-0604, P-0605, P-0606 (ii in **Figure 2**)

The characteristics of the secondary water pump are crucial, as it is the main positive pressure source within the system. For this reason, it determines the thermohydraulic characteristics of the system to a large degree.

The standard pump element found in Flownex® was found to be inferior to the more comprehensive variable speed pump element found in the Flownex SE 8.1.10 software. It was therefore decided to employ the variable speed pump element, but keep it either at standstill or running at 1 475 rpm. Data available was the Net Positive Suction Head (NPSH), hydraulic efficiency, the kilowatts as input and the total head in metres of water. Data additionally required was the heat fraction, the electrical efficiency of the motor and the mechanical efficiency of the pump.

To determine the values of the abovementioned requirements, an assumption had to be made in terms of the average capacity of the pumps. The electrical efficiency is not known and, as the mechanical efficiency is a factor in the overall pump efficiency, the mechanical efficiency could not be determined. The heat fraction also varies with the capacity of the pump as it is a function of input power (kilowatt).

To address this, the assumption of an electrical efficiency had to be made. No data was available on whether the motors employed were synchronous or induction motors, but the motors are said to operate at 1 475 rpm. It is known that for induction and synchronous motors, the following holds true:

$$\boldsymbol{RPM_{synchronous} = 120 \times \frac{f}{p}} \quad [5]$$

$$\boldsymbol{RPM_{induction} = 120 \times \frac{f}{p} \times Slip\ Factor} \quad [6]$$

Where:

f = The supply frequency in this case is 50 Hz.

p = The number of poles in this case is 4.

From this, one can determine that this is not a synchronous motor, as the given rpm is 1 475. The slip factor can subsequently be calculated as:

$$\boldsymbol{Slip\ factor = \frac{RPM_{induction}}{RPM_{synchronous}} = \frac{1475}{1500} = 0.983} \quad [7]$$

It was found that the recorded speed was not reached for any combination of poles and an operating frequency of 50 Hz. It is therefore assumed that an induction motor is employed, as the general rule for calculating the speed of a synchronous motor is not obeyed.

The electrical efficiency was assumed to be 91.7%, based on National Electrical Manufacturers Association (NEMA) design tables for standard efficiency motors (30). From this, the mechanical efficiency could be calculated based on Equation 8, as found in the Flownex Library Manual (8).

$$\boldsymbol{\dot{P}_e = \frac{\dot{P}}{\eta_m \eta_e}} \quad [8]$$

Since both the electrical power (31) and the power absorbed is known (19) for a specific duty point, the mechanical efficiency can be calculated from the above formula.

The final input required is the heat fraction, which is best described as the part of the generated heat that is transferred to the working fluid due to the mechanical and electrical inefficiencies. This is very difficult to establish if there are no temperature measurements before the water enters the pump and as it exits, as the formula below demonstrates (8).

$$\boldsymbol{\dot{Q}_H = H_f(1 - \eta_m \eta_e)\frac{\Delta p_0 \dot{Q}}{\eta_m \eta_e \eta_h} = H_f(1 - \eta_m \eta_e)\dot{P}_e} \quad [9]$$

If the before and after temperatures are known, the added heat could be easily be determined as follows (6):

$$\boldsymbol{\dot{Q} = \dot{m} C_p \Delta T} \quad [10]$$

Where:

C	=	Heat capacity rate (kJ/kg.K)
$\dot{Q}$	=	Heat transfer rate (kW)
$\dot{m}$	=	Mass flow rate (kg/s)
T	=	Temperature (K)

As this data is not available, the value of the heat fraction had to be estimated for the specific configuration. The Flownex® software specialists recommended a numerical value of 0.85 (32).

Derating

It was noticed that, from available data on the pressure nodes before and after the pump and available flow data for the pumps, the corresponding pressure drops on the pump curves overestimated the actual delivered flow rates. This pointed to losses that were not encountered when the pump curves were issued (19). The following is based on the assumption that the measured values were obtained using measuring equipment that is calibrated to set standards.

The logical course of action was to effectively derate the pumps as typically done in industry on equipment used for non-standard fluids. It was assumed, as with slurry derating, that a percentage reduction on the pressure curve would be implemented. This percentage reduction was determined by comparing the actual performance measurements to the measurements gained from running the specific pressure curves in Flownex®.

The deviation of the current set-up to the predicted behaviour, as measured when the latest curves were issued, are shown in the **Table 3**. The performance for pump P-0606 is omitted as the available data was insufficient to determine operating pressure differentials as this unit is typically on stand-by.

Table 3: Reactor secondary water pump derating percentage

Pump	Performance differential (%)
P-0601	10.85
P-0604	11.76
P-0605	9.27

The table points to a performance differential that does not vary too much from pump to pump. This would lead one to believe that the diminished performance is potentially due to expected timely wear or possible impeller modifications, and not to mechanical failure.

Y-joint

Designation: Juncture of line 500-06-WCCG-1048 and continuation of 300-06-WCCG-1047 (① in **Figure 5**)

The Y-joint that is situated after the reactor secondary water pump is a non-standard joint manufactured for the system. Due to the direction of the flow (two streams are joining), the non-standard shape of the joint and the skewed relation of flow rates through the conjoining legs, an appropriate formula had to be incorporated to approximate the pressure loss over the joint.

Before solving the pressure loss coefficients, the different combinations in which three of the four pumps can operate and the influence this will have on the pressure drop through the Y-joint have to be determined. As can be seen in **Figure 6**, there is only two options in terms of pure flow rate through the Y-joint, as a minimum of three pumps are required for effective operation. The fourth pump is assumed to be a backup unit.

If the flow rate is assumed to be equal through all operational pumps and it is suggested by the arbitrary denominator of “X” kg/s, the flow would be as summarised in **Table 4**.

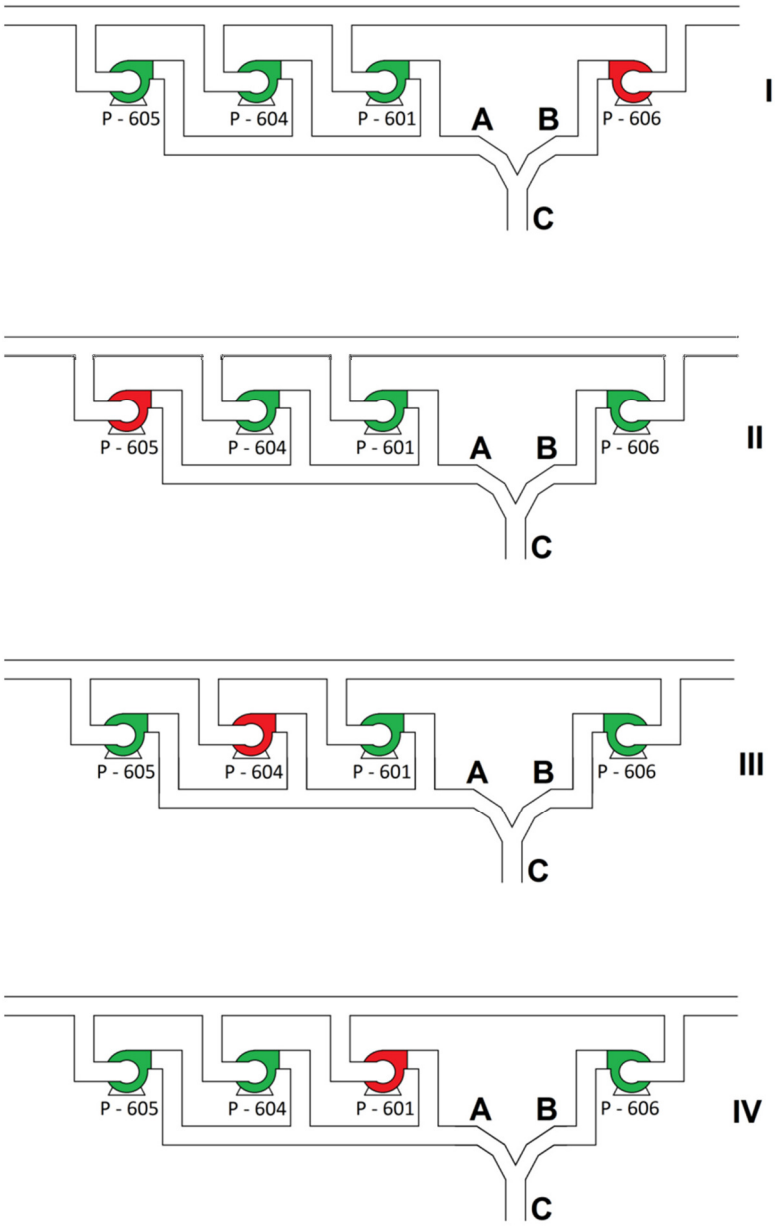

Figure 6: Y-joint flow scenarios

Table 4: Y-joint effective flow

Scenario	Leg A flow	Leg B flow	Leg C flow
I	3X	0	3X
II	2X	X	3X
III	2X	X	3X
IV	2X	X	3X

The flow rates employed were based on assumed operating ranges to determine the constant K-factors through the pipe bends. The approach assumes calculated K-factors for each of the two legs and, it would apply the relative loss coefficient K of the various legs, depending on the configuration of the pumps.

The approach employed to determine the loss coefficient K was based on the formula below with reference to **Figure 7** (33).

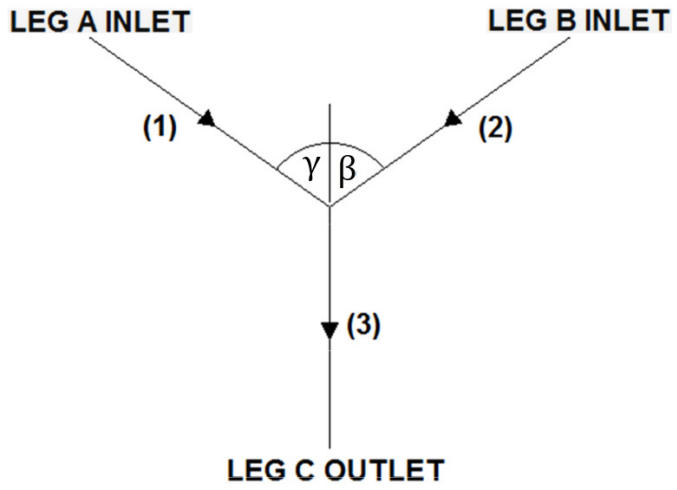

Figure 7: Y-joint schematic

$$K_{13} = 0.97\left(\frac{v_1}{v_3}\right)^2 + 1 - 2\left(\left(\frac{v_1}{v_3}\right)\frac{Q_1}{Q_3}cos\gamma' + \left(\frac{v_2}{v_3}\right)\frac{Q_2}{Q_3}cos\beta'\right) \quad [11]$$

$$K_{23} = 0.97\left(\frac{v_2}{v_3}\right)^2 + 1 - 2\left(\left(\frac{v_2}{v_3}\right)\frac{Q_2}{Q_3}cos\gamma' + \left(\frac{v_1}{v_3}\right)\frac{Q_1}{Q_3}cos\beta'\right) \quad [12]$$

Where:

$$\gamma' = 1.41\gamma - 0.00594\gamma^2 \quad [13]$$

$$\beta' = 1.41\beta - 0.00594\beta^2 \quad [14]$$

Substituting the relevant values yields loss coefficients for the junction as seen in **Table 5** and **Table 6**.

Pumps active: P-0601, P-0604 and P-0605 as seen in **Table 5**.

Table 5: Y-joint loss coefficient default arrangement

Loss coefficients	Value
K_{13}	0.723
K_{23}	-0.247

It is noted that, when employing equation 12, K_{23} has a negative value which therefore implies a pressure rise value, but due to the zero flow velocity through the leg, it has no effect on the actual pressure distribution within the system.

Pumps active: P-0606, P-0601 and P-0604/P-0604 and P-0605/P-0601 and P- 0605 as seen in **Table 6**

Table 6: Y-joint loss coefficient alternative arrangement

Loss coefficients	Value
K_{13}	0.738
K_{23}	0.415

Primary heat exchanger

Designation: E-0101, E-0102, E-0103, E-0104 (v in **Figure 2**)

Based on the general empirical relationship of Equation 4, it can safely be assumed that a value of 2 for α is to be used for the primary side of the heat exchanger, as it is predominantly pipe flow. Since the temperatures are also well below boiling point, the value of β can be assumed to be a constant 1. This simplifies the calculations, as there is only one unknown, namely C_k. Although there is limited data available on the pressure drops found with associated equipment flow rates, the values of C_k could still be established within reasonable margins of error.

The value of C_k was found to be with reference values from (34), as listed in **Table 7**:

Table 7: Primary heat exchanger empirical pressure drop constants

Pressure loss constants	Value
C_k	1 157.87
α	2

Dividing flow branch

Designation: Juncture of line 450-06-WCCG-1071 and continuation of 300-06-WCCG-1074 (② in **Figure 5**)

As with the Y-joint mentioned earlier, it was deemed necessary to employ specialised formulae to determine the effects of the branch on the loss coefficients K. As all four heat exchangers are always operational, the distribution of the flow ratios was assumed to remain constant, and therefore, only a single flow scenario was deemed necessary.

Employing equations 15 and 16 from (33), one can determine the effect of the branch on the loss coefficient.

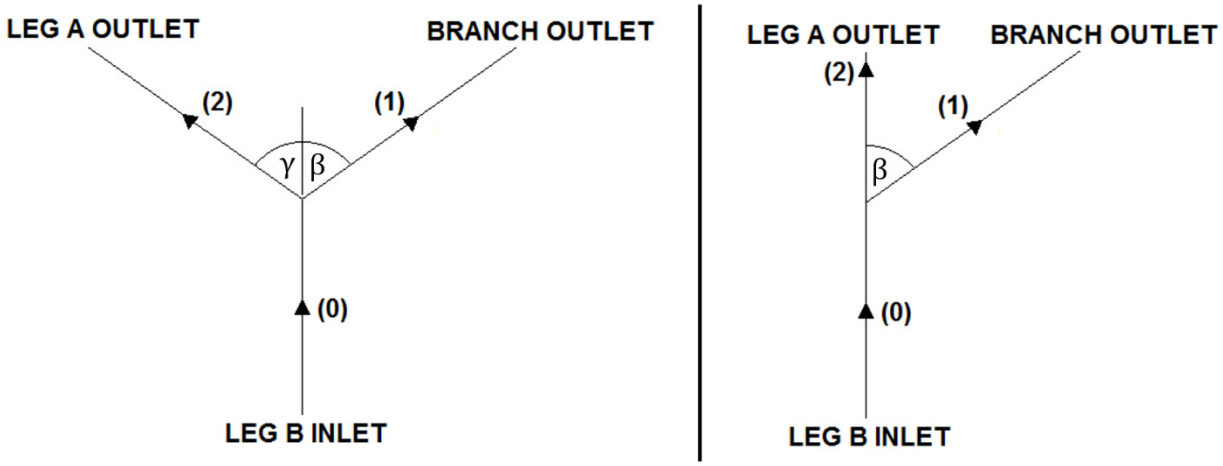

Figure 8: Dividing branch flow schematic

$$K_{01} = \lambda_1 + (2\lambda_2 - \lambda_1)\left(\frac{V_1}{V_0}\right)^2 - 2\lambda_2\left(\frac{V_1}{V_0}\right)\cos\gamma' \quad [15]$$

$$K_{02} = \lambda_1 + (2\lambda_2 - \lambda_1)\left(\frac{V_2}{V_0}\right)^2 - 2\lambda_2\left(\frac{V_2}{V_0}\right)\cos\beta' \quad [16]$$

Where:

$$\gamma' = 1.41\gamma - 0.00594\gamma^2 \quad [4]$$

$$\beta' = 1.41\beta - 0.00594\beta^2 \quad [5]$$

$$\lambda_1 = 0.0712\gamma^{0.7141} + 0.37 \; for \; \gamma < 22.5° \quad [19.1]$$

$$\lambda_1 = 1.0 \; for \; \gamma \geq 22.5° \quad [19.2]$$

$$\lambda_2 = 0.0592\gamma^{0.7029} + 0.37 \; for \; \gamma < 22.5° \quad [20.1]$$

$$\lambda_2 = 0.9 \; for \; \gamma \geq 22.5° \quad [20.2]$$

$$\lambda_1 = 0.0712\beta^{0.7141} + 0.37 \; for \; \beta < 22.5° \quad [19.3]$$

$$\lambda_1 = 1.0 \; for \; \beta \geq 22.5° \quad [19.4]$$

$$\lambda_2 = 0.0592\beta^{0.7029} + 0.37 \; for \; \beta < 22.5° \quad [20.3]$$

$$\lambda_2 = 0.9 \; for \; \beta \geq 22.5° \quad [20.4]$$

Substituting the relevant values yields the results of the loss coefficients for the dividing flow branch as seen in **Table 8**:

Table 8: Dividing flow branch loss coefficients

Loss coefficients	Value
K_{01}	0.639
K_{02}	0.093

Ball collector

Designation: T-0610 (viii in **Figure 2**)

The ball collector is part of an on-line tube-cleaning system that was pioneered by Trapogge® (19). The system allows small foam rubber balls to circulate through the tubes of the primary heat exchangers to reduce fouling and increase the equipment life and efficiency of the heat exchangers.

The function of the ball collector is to separate the foam rubber balls from the main coolant line and direct the balls to facilitate recirculation.

As there was virtually no technical data available on the ball collector, existing photographs and estimated measuring techniques were employed to construct a three-dimensional model to import to the CFD software to obtain pressure loss figures within the expected range of flow conditions. The flow range varied from 530 kg/s to 780 kg/s and yielded the results in **Table 9** when applied to the empirical pressure loss equation employed by the Flownex® custom loss element. The same principles were applied as with the ball strainer.

Table 9: Ball catcher empirical pressure drop constants

Pressure loss constants	Value
C_k	13.886
α	2.038

Recirculation pump

Designation: P-0608 (vii in **Figure 2**)

There was limited technical data about the pump curves and performance charts. It was therefore necessary to use the technical data from an alternative pump with similar expected characteristics and expected flow rate capabilities.

The pump selected to mimic the current set-up was the KSB Etabloc N 65-200 (35), the parameters of which were employed on the standard Flownex® pump element.

Ball strainer

Designation: C-0609 (vi in **Figure 2**)

The ball strainer forms part of the Trapogge® system (19) that is briefly explained above. It is a strainer from where the foam rubber cleaning balls can be collected and inspected by the operator. Under normal operating conditions, the strainer allows unobstructed passage of the foam rubber balls. This was the chosen arrangement to analyse the strainer's associated pressure drop. As there was no technical data available on the associated pressure drops through the ball collector, a CFD model had to be constructed and subjected to numerous flow conditions to accurately simulate the macro effect of the component within the system. The obtained solution through CFD, was evaluated and compared within known boundaries along with applying best practices in CFD simulation. This approach was also applied to all other CFD modelled components.

Detailed sketches, along with measurements and basic assumptions that follow good engineering practice, were employed to reconstruct a virtual model of the ball collector. This was then subjected to estimated flow rates, as within the capabilities of the recirculation pump P-0608.

The data was then applied to a custom loss element, as found in the Flownex® program, which is subject to the general empirical pressure loss formula.

The results for a flow rate range of 9 to 13 kg/s with the resulting flow loss constants are tabulated in **Table 10**.

Table 10: Ball strainer empirical pressure drop constants

Pressure loss constants	Value
C_k	78 088.623
α	1.974

200 mm Y-strainer

Designation: Y-0602

No technical data was available on the Y-strainer employed on-line 200-06-WCCG-1051 (③ in **Figure 5**). Data on Y-strainers of similar construction was incorporated to attain pressure loss data as per the Sure Flow Equipment Inc. (36). The data available was incorporated into the custom loss flow element employed by the Flownex® software, and analytical manipulation of the attained data yielded the following constants for the custom loss flow element over a mass flow range of 25 up to 314 kg/s, as tabulated in **Table 11**.

Table 11: 200 mm Sure Flow basket Y-strainer empirical pressure loss constants

Pressure loss constants	Value
C_k	1 047.474
α	1.866

As with the basket strainers, there is an expected difference between the pressure drop values of a modern Y-strainer and that which is employed in the system. Employing the same approach with regard to the characteristic flow through the Y-strainer, the achieved value for the empirical pressure loss data could be determined as seen in **Table 12**.

Table 12: Actual 200 mm Y-strainer empirical pressure loss constants

Pressure loss constants	Value
C_k	5 700
α	1.866

Pool heat exchanger

Designation: E-0301 (iii in **Figure 3**)

Based on the general empirical relationship of Equation 4, it can safely be assumed that a value of 2 for α is to be used for the primary side of the heat exchanger, as it is predominantly pipe flow. Since the temperatures are also well short of boiling point, the value of β can be assumed to be a constant 1. This simplifies the calculations, as there is now only one unknown, namely C_k, within the system. As with the primary heat exchanger, the value of the constant $C_k$could be determined with relative ease.

The value of C_k was therefore found to be as listed in **Table 13**.

Table 13: Pool heat exchanger empirical pressure loss constants

Pressure loss constants	Value
C_k	7 268.98
α	2

L-bend

Designation: Juncture of line 400-06-WCCG-1049 and 150-06-WCCG-1054 (④ in **Figure 5**)

The significance of this juncture opposed to any other bend found in the system is the abrupt change in bend diameter. The diameter is significantly reduced from 400 mm to 150 mm in what is essentially a blanked off T-junction. This is a non- standard reducer, and due to the limited technical information available on the bend, assumptions had to be made based on the encountered pressure drops, best engineering practices and most probable solution. Various models were set up and run with the CFD software, with the final result based on the most probable of the

geometric solutions.

In the Flownex® model, the element was once again replaced by the custom loss element found in the Flownex® software to allow accurate representation of the hydraulic effects of the bend. The constants according the empirical pressure loss equation are shown in **Table 14**.

Table 14: L-bend empirical pressure loss constants

Pressure loss constants	Value
C_k	2 229.014
α	1.976

80 mm Y-strainer

Designation: Y-0603

No technical data was available on the Y-strainer employed on-line 150-06-WCCG-1054 (⑤ in **Figure 5**). Data on Y-strainers of similar construction was incorporated to attain pressure loss data as per Sure Flow Equipment Inc. (36). The data available was incorporated into the custom loss flow element employed by the Flownex® software and analytical manipulation of the attained data yielded the following constants, as can be seen in **Table 15** for the custom loss flow element over a mass flow range of 14 kg/s up to 70 kg/s.

Table 15: 80 mm Sure Flow Y-strainer empirical pressure loss constants

Pressure loss constants	Value
C_k	51 282.43
α	1.989

The assumption that the Y-strainers installed in the secondary cooling system have similar pressure drop characteristics to that which is typically supplied by the Sure Flow Equipment Company is incorrect, as discussed in 4.1.1 (basket strainers).

The same argument is followed as in 4.1.1 (basket strainers), as the internal dimensions of the currently employed Y-strainer is not available to determine the required characteristics through CFD analysis. The type of flow curve, as represented in the general empirical formula as α, was employed from the Sure Flow strainers, as it is assumed that the characteristic flow should be relatively the same due to shared design principles. The effective pressure drop would therefore be determined by varying the value of C_k to allow for adequate flow between known values within the system. The achieved value is paradoxical, as the lower value of C_k allows for sufficient flow conditions, but forces a smaller pressure drop, which contradicts pressure data for this line. A possible explanation is given in Section 5.4.

The achieved value for the empirical pressure loss data was determined as shown in **Table 16.**

Table 16: 80 mm strainer (Y-0603) empirical pressure loss constants

Pressure loss constants	Value
C_k	30 000
α	1.989

Fan coil units

Designation: E-0618, E-0619, E-0620 (vi in **Figure 4**)

The fan coil units are cross-flow heat exchangers that provide cooling to the primary pumps of the reactor. There is currently no record or technical data available of the characteristics of these cross-flow heat exchangers. All that is known is that it utilises chilled water from the secondary system to cool the rooms through forced convection. The internal arrangements are unknown to the operational staff and, due to their positions, access for closer inspection was not possible.

A more simplistic approach was undertaken to circumvent the apparent lack of data. Thermal measuring instruments were employed to check the difference between the inlet and the outlet pipe surface temperatures of the fan coils. It is then possible to assume that, through conduction, the resistance provided by elements such as the fouling, tubing and paint, was similar on the inlet and outlet sides. The recorded change

in temperature of the pipe surface would be the same as the bulk temperature change of the water inside the tube at steady state. Further assumptions were based on the flow rates achieved through the heat exchangers. This was calculated as the average of the three heat exchangers (the difference between the flow rates delivered by the pump and the chiller units). From this data and the assumption of steady flow, the first law of thermodynamics was employed to determine the energy balance through Equation 21 (24). Based on the abovementioned assumptions, the work could then be calculated and inserted as a pressure loss element with a fixed heat input.

$$\dot{\boldsymbol{Q}} = \dot{\boldsymbol{m}}\boldsymbol{C_p}\Delta\boldsymbol{T} \qquad [21]$$

Where:

C	=	Heat capacity rate (kJ/kg.K)
$\dot{Q}$	=	Heat transfer rate (kW)
$\dot{m}$	=	Mass flow rate (kg/s)
T	=	Temperature (K)

In terms of the associated pressure drop through the elements, the lack of data once again prompted the comparison of the heat exchanger's effect on the system as a whole with established values measured elsewhere. As the flow rates encountered in this line is relatively small and could reasonably even be neglected, the estimation using the Flownex® designer (37) to fit the appropriate values within reasonable bounds was deemed a good approach. The calculation is simplified by the reasonable assumption that tube flow is encountered within the unit, leaving the empirical loss equation with only one unsolved constant, as it is reasonable to assume α as 2 for tube flow.

The empirical constant C_k cannot be solved due to the lack of performance and physical data. This does not pose a problem, as the effect of C_k on the overall system would be negligible due to the relatively low flow rates. For an arbitrary change of 1 kPa through a fan coil unit, the corresponding value of C_k would have to be in the range of 7 672 748. This is a very high value and unlikely at best due to the typical construction of similar units. In the unlikely event that the value of C_k is abnormally high, the associated flow rates are so low that it ensures a virtual negligible effect on the system as a whole. It was therefore decided to settle on a reasonable value of 500 for C_k, as can be seen in **Table 17**.

Table 17: Fan coil units' empirical pressure loss data

Pressure loss constants	Value
C_k	500
α	2

Carrier chiller unit

Designation: X-1401 (v in **Figure 4**)

The Carrier chiller unit is employed to cool air throughout specific areas in the building by making use of chilled water as a heat sink. Insufficient data was available to fully construct the model, as this is a non-critical, low-priority element within the system where no data logging is done on the inlets and outlets of the particular heat exchanger.

To integrate the data with the simulation program, a custom loss element had to be implemented. The available data had to be transformed to fit the empirical loss equation as mentioned above. To do this, the available data depicted the net cooling capacity, the compressor power input, the effective power input, the evaporator water pressure drop and the condenser water pressure drop. This data was selected for a specific condenser inlet water temperature and varying exit cooler temperature.

The evaporator water flow, the condenser water flow and the total heat rejection was successively calculated. From this, the data could be arranged to calculate the constants of the empirical pressure loss in Equation 4 by solving for C_k by varying values for α. At the value of α where the standard deviation for the corresponding values for C_k was at a minimum, the constants α and C_k were eventually calculated. C_k was determined as the average of the different values of C_k at different flow rates for that specific α. The constants acquired through this exhaustive process can be found in **Table 18**.

Table 18: Carrier chiller unit empirical pressure loss constants

Pressure loss constants	Value
C_k	113 310
α	1.765

To address the heat input variable within the custom loss element, the heat generated had to be considered. The heat input at the condenser side is the cumulative value of the net cooling capacity and the partial compressor power input. Due to losses to the environment and the mechanical losses through the compressor unit, it is very difficult to determine the actual heat input into the working fluid at the secondary cooling side. A lack of detailed information restricted this approach and an alternative had to be sought.

According to the manufacturer, a change of 5 kelvin can be expected between the inlet and outlet of the condenser unit, irrespective of the condenser inlet water temperature or the cooler outlet temperature. This claim was substantiated by an in-operation test according to data obtained from Necsa (37, 38). This data could be used in conjunction with the Flownex® designer as an equality constraint, with the heat input as the independent variable. The Flownex® designer would then determine the actual heat input for that specific scenario in terms of flow rate. Since the flow rate is marginally, yet constantly varying throughout the element in reality, the accuracy of the heat input is relative to the conditions encountered, but since the relative flow volumes are small in relation to the total system, the constant value was assumed sufficient for the purpose of the study. The final value of the heat power input was determined as 220.326 kW in the secondary system.

Daikin chiller unit

Designation: X-1402 (iii in **Figure 4**)

The Daikin chiller unit, as for the abovementioned Carrier unit, is employed to provide cool air throughout specific areas in the building. The Daikin unit is significantly older than the Carrier unit and it is mostly used as a backup system when the Carrier is out of service. Occasionally, the system is switched over to the Daikin unit to ensure operational availability.

Due to the age and total lack of available data on the system, assumptions had to be made in terms of pressure loss and performance. As there is no marked characteristic change in volume flow in the system during a typical year, which is a reasonable time that the Daikin chiller is in operation, it could be inferred that the flow rates through that part of the system has been relatively unchanged. This allows for the assumption that, since the heat load requirements have not changed, the system should be very similar to the Carrier in terms of performance. The construction that most resembles the current Daikin chiller is that of Daikin model UWD1700DY1. This is a modern product and even though it is very similar in terms of physical specification, the difference in performance is significant. Due to lack of data and infrequent use, it was decided that the characteristics in terms of pressure drop and heat input would be based on the Carrier chiller system.

4.2 Subsystems

Flownex® does not require subsystem analysis, as it performs system analysis from individual structures and components. The only subsystem that requires separate analysis is the cooling towers, as the complex nature of this subsystem cannot be effectively modelled using current Flownex® capabilities.

4.2.1 Cooling towers

The cooling towers are approached in a different manner, as they are not only subject to varying flow conditions, but also to different ambient temperatures. This influences the performance of the cooling towers, which yield- an ever more complex system.

The approach employed to overcome the different scenarios would be to run a large number of simulations and establish a trend of cooling tower performance by employing known variables. Due to the virtually infinite psychrometric combinations, setting up such a table would be a futile exercise, as integration into the system would not only be difficult to achieve, but also overly labour intensive. To address this situation, a model of the cooling tower was created to allow for variable inputs, generating case-specific data inputs for the Flownex® model. The generated model would then be compared to existing values on the cooling tower and performance (39). The existing data on the cooling towers are somewhat doubted due to the “perfect” values attained and could be ascribed to the accuracy of the installed measuring equipment. Some of

the variables are discussed, and the various systems are characterised based on input values from existing Necsa documentation.

Even though it is not a variable, the fan characteristics of the cooling towers had to be determined, as the information was not readily available. The data required for the input variables for the software was attained from internal Necsa documents. (40)

The original manufacturer could not supply data for the study, so a leading manufacturer's catalogue was employed to find a viable alternative. The software, when inserting the relevant variables, produced the results attached in Appendix VII.

This data was then employed to set up the model of the cooling towers, with the results subsequently compared to that of the original manufacturer, as can be seen in **Table 19**.

Table 19: Cooling tower performance comparison

	Original manufacturer	**Model specifications**
Outlet water temperature (OWT)	25 °C	24.69 °C
Heat rejected	4.00 MW	4.14 MW

For the Flownex® model, all constants attained from the above were employed as in Appendix VII, with the only variables being the ambient temperature, flow rate and inlet water temperature, which were adjusted to comply with the Flownex® model inputs and results.

4.3 Synthesis

This section describes the results attained from the integrated system, which includes all data generated under structures and components and subsystems, as well as all other supplied information. The results for the system at all points are attached in Appendix III. Only the results that are required to verify the total model follow.

4.3.1 Method

As described earlier, the model is based on Flownex®, which executes a steady-state analysis. To yield comparable results, the minimum amount of readings from within the actual system had to be incorporated into the model as inputs. The model was then run using the given input parameters and compared to all other existing data points taken under similar operating conditions. The Flownex® results would then be compared with high-quality experimental readings.

4.4 Simulation results

To aid the reader, the results of the simulation, the various system components and associated numbering have been graphically represented in **Figure 9,** which gives an overall view of the integrated system. To simplify the system, it has been divided into the following subsystems:

- Cooling tower (**Figure 10**)
- Primary heat exchanger (**Figure 11**)
- Fan coil and chiller units (**Figure 12**)
- Pool heat exchanger (**Figure 13**)
- Reactor heat exchanger (**Figure 14**)
- Tube-cleaning subsystem (**Figure 15**)

With each of the subsections, the figure specifies numerical points and flow directions at each major component. These points are reference points at which available data is presented in the corresponding table under the given number.

Within the table, the item description is given, followed by the Necsa designation. A target value (based on actual recorded values) is given if available. The achieved value from the model and the relative error are given if relevant.

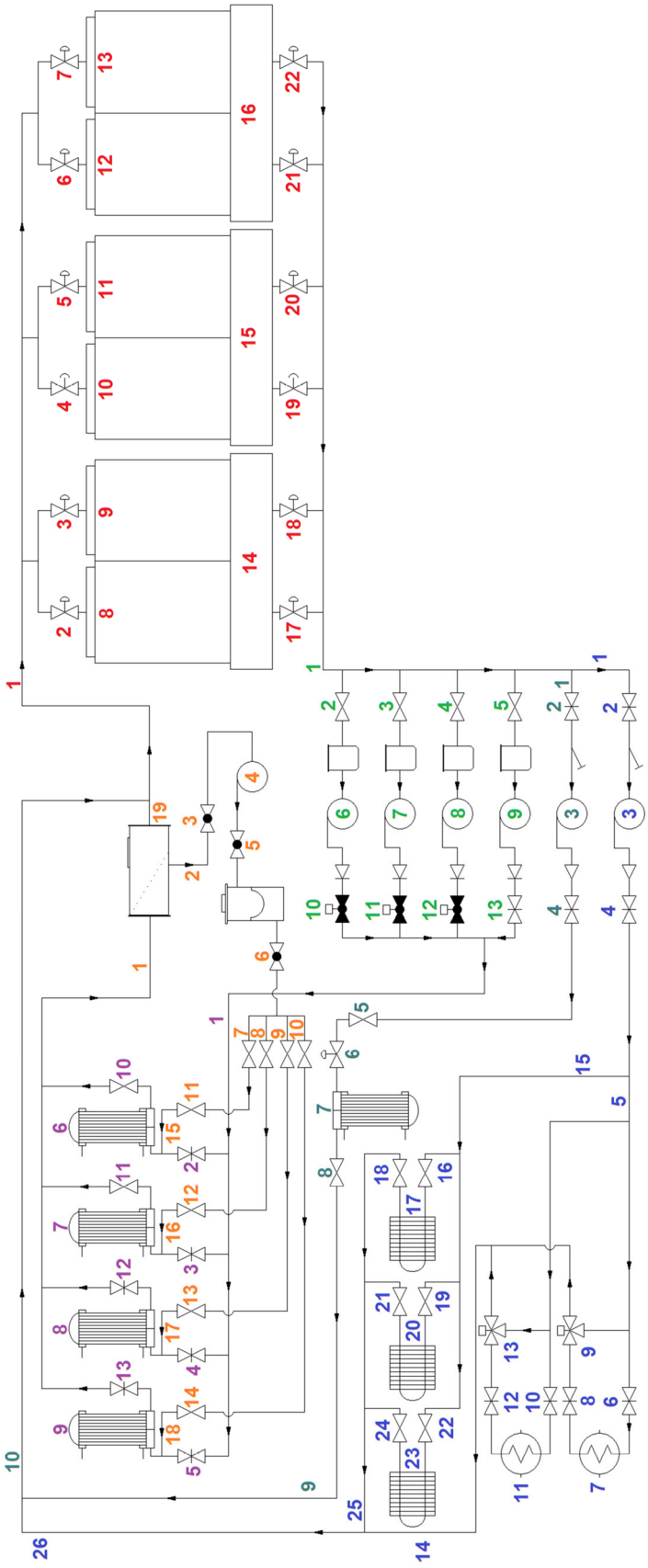

Figure 9: Secondary cooling system schematic

(19)

4.4.1 Cooling tower subsystem

The cooling tower subsystem, as depicted in **Figure 10**, and the inlet condition are specified by point 1. The varying degrees of the inlet valve openings are represented by designators 2 to 7. The flow conditions of the spray manifolds are given from designators 8 to 13. The water level in each communal basin is designated by the labels 14 to 16. The varying degrees of the outlet valve openings are represented by designators 17 to 22. All corresponding values are presented in **Table 20**.

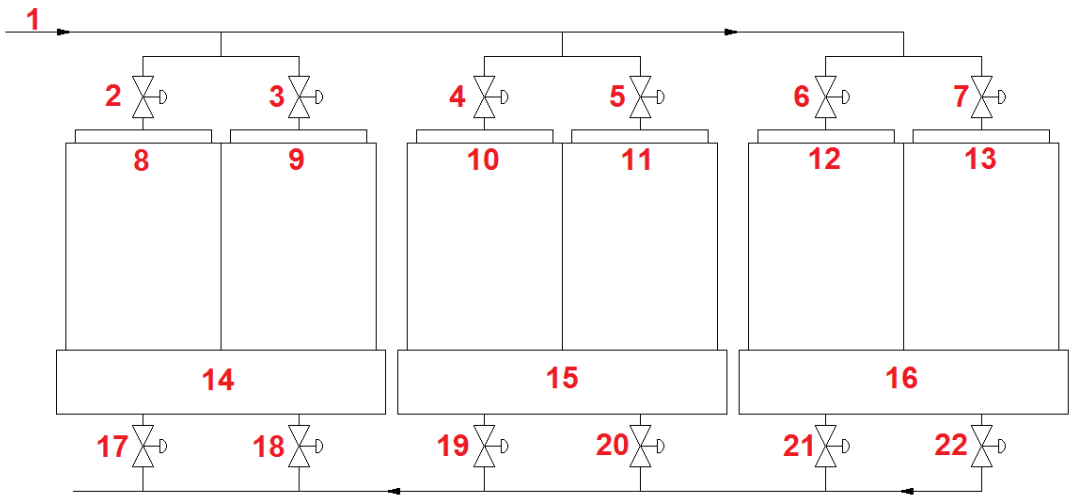

Figure 10: Cooling tower subsystem schematic

Table 20: Cooling tower subsystem results

No	Description	Unit	Measured	Simulation	Error (%)	Note
1	**Cooling tower main inlet pipe**					
	500-06-WCCG-1002					
	Total temperature	℃		31.6		
	Total mass flow rate	kg/s		617.1		
	Static pressure	kPa		243.6		
2	**West cooling tower inlet valve**					
	V-0605					
	Fraction open			1.00		
3	**West cooling tower inlet valve**					
	V-0606					
	Fraction open			1.00		
4	**Centre cooling tower inlet**					
	V-0649					
	Fraction open			0.48		
5	**Centre cooling tower inlet**					
	V-0650					
	Fraction open			0.48		
6	**East cooling tower inlet valve**					
	V-0647					

No	Description	Unit	Measured	Simulation	Error (%)	Note
	Fraction open			0		
7	**East cooling tower inlet valve**					
	V-0648					
	Fraction open			0		
8	**West cooling tower inlet line**					
	400-06-WCCG-1036					
	Total temperature	℃		31.672		
	Total mass flow rate	kg/s		154.297		
	Static pressure	kPa		143.770		1
9	**West cooling tower inlet line**					
	400-06-WCCG-1035					
	Total temperature	℃		31.672		
	Total mass flow rate	kg/s		154.297		
	Static pressure	kPa		143.770		1
10	**Centre cooling tower inlet line**					
	400-06-WCCG-1026					
	Total temperature	℃		31.672		
	Total mass flow rate	kg/s		154.298		
	Static pressure	kPa		143.770		1
11	**Centre cooling tower inlet line**					
	400-06-WCCG-1025					
	Total temperature	℃		31.672		
	Total mass flow rate	kg/s		154.298		
	Static pressure	kPa		143.770		1
12	**East cooling tower inlet line**					
	400-06-WCCG-1016					
	Total temperature	℃		25.002		
	Total mass flow rate	kg/s		0		
	Static pressure	kPa		87.180		1
13	**East cooling tower inlet line**					
	400-06-WCCG-1015					
	Total temperature	℃		25.002		
	Total mass flow rate	kg/s		0		
	Static pressure	kPa		87.180		1
14	**West cooling tower basin**					
	W601					
	Water level	m		2.028		
	Total temperature	℃		24.911		
	Total mass flow rate	kg/s		308.595		
	Static pressure (surface)	kPa	87.178	87.180	0.002	
15	**Centre cooling tower basin**					
	W602					
	Water level	m		2.0648		
	Total temperature	℃		24.911		
	Total mass flow rate	kg/s		154.298		
	Static pressure (surface)	kPa	87.178	87.180	0.002	
16	**East cooling tower basin**					

No	Description	Unit	Measured	Simulation	Error (%)	Note
	W603					
	Water level	m		2.099		
	Total temperature	℃		24.911		
	Total mass flow rate	kg/s		154.298		
	Static pressure (surface)	kPa	87.178	87.180	0.002	
17	**West cooling tower inlet valve**					
	V-0632					
	Fraction open			1		
	Total mass flow rate	kg/s		128.752		
18	**West cooling tower outlet**					
	V-0643					
	Fraction open			1.000		
	Total mass flow rate	kg/s		179.843		
19	**Centre cooling tower outlet**					
	V-0634					
	Fraction open			1		
	Total mass flow rate	kg/s		57.191		
20	**Centre cooling tower outlet**					
	V-0640					
	Fraction open			1.000		
	Total mass flow rate	kg/s		97.107		
21	**East cooling tower outlet valve**					
	V-0636					
	Fraction open			1.000		
	Total mass flow rate	kg/s		77.253		
22	**East cooling tower outlet valve**					
	V-0635					
	Fraction open			1.000		
	Total mass flow rate	kg/s		77.045		

Note:

1. Addressed in Section 5.3.

4.4.2 Primary heat exchanger pump subsystem

For the primary heat exchanger pump subsystem, the inlet condition is specified by point 1, as depicted in **Figure 11**. The varying degrees of the inlet valve openings is represented by designators 2 to 5. The flow conditions and pressure rises of the individual pumps are given from designators 6 to 9. The varying degrees of the outlet valve openings is represented by designators 10 to 13. All corresponding values are presented in **Table 21**.

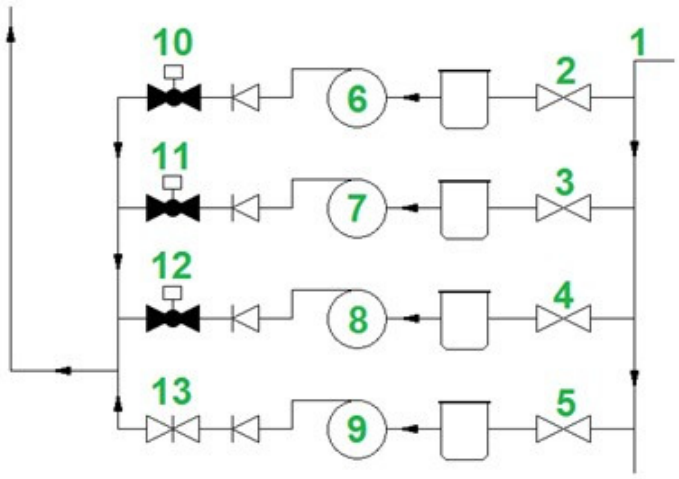

Figure 11: Primary heat exchanger pump subsystem schematic

Table 21: Primary heat exchanger pump subsystem results

No	Description	Unit	Measured	Simulation	Error (%)	Note
1	**Heat exchanger pump room**					
	600-06-WCCG-1001					
	Total temperature	℃		24.913		
	Total mass flow rate	kg/s		617.19		
	Static pressure	kPa		112.276		
2	**Pump P-0605 inlet valve**					
	V-0627					
	Fraction open			1		
3	**Pump P-0604 inlet valve**					
	V-0630					
	Fraction open			1		
4	**Pump P-0601 inlet valve**					
	V-0607					
	Fraction open			1		
5	**Pump P-0606 inlet valve**					
	V-0674					
	Valve angle	Deg		0		
6	**Pump P-0605**					
	P-0605					

No	Description	Unit	Measured	Simulation	Error (%)	Note
	Static temperature	℃		24.918		
	Total mass flow rate	kg/s		189.442		
	Inlet pressure	kPa	79.600	74.869	5.943	
	Outlet pressure	kPa	301.900	296.639	1.743	
7	**Pump P-0604**					
	P-0604					
	Static temperature	℃		24.917		
	Total mass flow rate	kg/s		185.232		
	Inlet pressure	kPa	77.300	76.932	0.478	
	Outlet pressure	kPa	295.900	296.114	0.072	
8	**Pump P-0601**					
	P-0601					
	Static temperature	℃		24.917		
	Total mass flow rate	kg/s		190.296		
	Inlet pressure	kPa	77.500	76.400	1.419	
	Outlet pressure	kPa	299.500	293.929	1.860	
9	**Pump P-0606**					
	P-0606					
	Static temperature	℃	-	-		1
	Total mass flow rate	kg/s	-	-		1
	Inlet pressure	kPa	-	-		1
	Outlet pressure	kPa	-	-		1
10	**Pump P-0605 outlet valve**					
	V-0269					
	Fraction open			1.000		
11	**Pump P-0604 outlet valve**					
	V-0622					
	Fraction open			1.000		
12	**Pump P-0601 outlet valve**					
	V-0602					
	Fraction open			1.000		
13	**Pump P-0606 outlet valve**					
	V-0676					
	Valve angle	Deg		0.000		

Note:

1. No flow through P-0606.

4.4.3 Fan coil and chiller water unit subsystem

For the fan coil and chiller water unit subsystem, the inlet condition is specified by point 1, as depicted in **Figure 12.** The degree of the inlet valve opening is represented by designator 2. The flow conditions and pressure rise of the pump are given designator 3. The outlet valve opening is represented by designator 4. The inlet condition to the chiller units is specified by point 5. Designators 6, 7, 8 and 9 represent the Carrier chiller's inlet valve position, the flow conditions at the chiller unit itself, the outlet valve condition and the bypass valve's flow direction respectively. Numbers 10 to 13 denote the same for the Daikin chiller unit. Point 14 refers to the outlet conditions of the chiller units. Point 15 is conversely the inlet conditions for the fan coil unit, with points 16, 17 and 18 denoting the inlet valve position, the flow conditions at the fan coil unit and the outlet valve condition, respectively, of the fan coil unit. Points 19 to 24 denote the same for the other two fan coil units. Point 25 is the achieved exit flow conditions of the fan coil units, with point 26 being the combined outlet flow of the chiller units and the fan coil units respectively. All corresponding values are presented in **Table 22**.

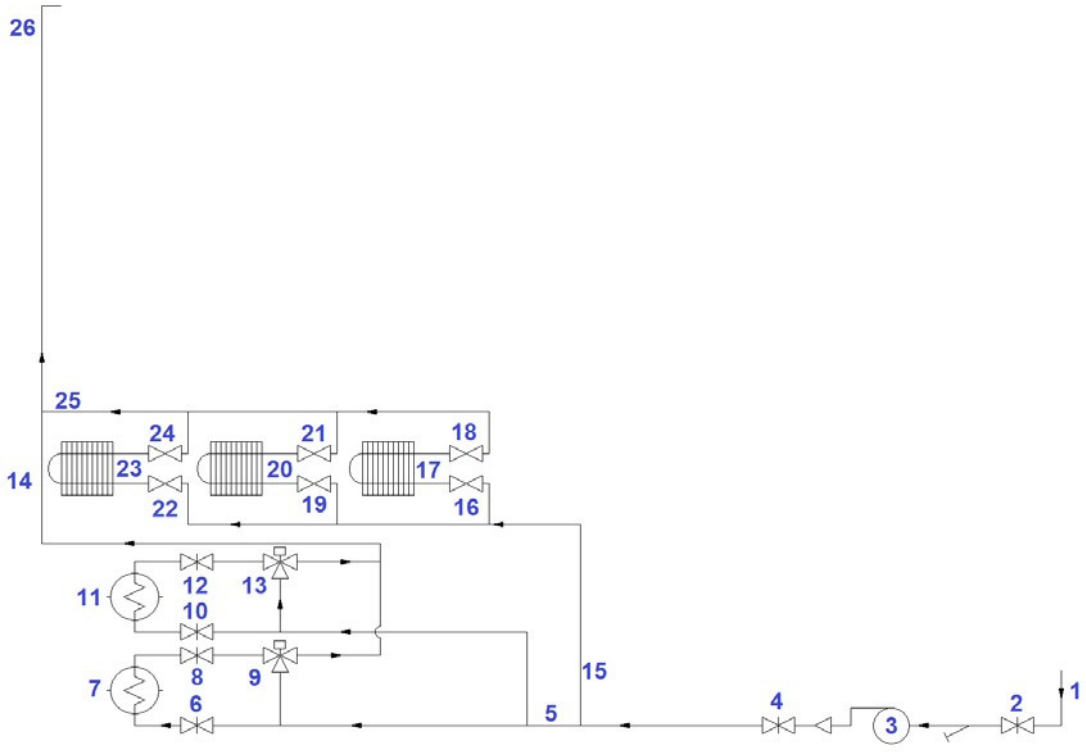

Figure 12: Fan coil and chiller water unit subsystem schematic

Table 22: Fan coil and chiller unit subsystem results

No	Description	Unit	Measured	Simulation	Error (%)	Note
1	**Fan coil unit and chiller unit**					
	150-06-WCCG-1054					
	Total temperature	℃		24.913		
	Total mass flow rate	kg/s		13.752		
	Static pressure	kPa		105.458		
2	**Pump P-0603 inlet valve**					
	V-0615					
	Valve angle	deg		90.000		
3	**Pump P-0603**					
	P-0603					
	Static temperature	℃		24.915		
	Total mass flow rate	kg/s	14.020	13.752	1.912	
	Inlet pressure	kPa		91.715		
	Outlet pressure	kPa	287.625	341.377	18.688	1
4	**Pump P-0603 outlet valve**					
	V-0617					
	Valve angle	deg		90.000		
5	**Chiller units water supply**					
	150-06-WCCG-1056					
	Total temperature	℃		24.963		
	Total mass flow rate	kg/s		10.384		
	Static pressure	kPa		266.575		
6	**Carrier inlet valve**					
	V-0687					
	Valve angle	deg		41.000		
7	**Carrier chiller unit**					
	X-1402					
	Inlet temperature	℃		24.971		
	Outlet temperature	℃	28.678	30.054	4.798	
	Total mass flow rate	kg/s	10.600	10.384	2.038	
	Inlet pressure	kPa		222.171		
	Outlet pressure	kPa		186.313		
8	**Carrier outlet valve**					
	V-0688					
	Valve angle	deg		90.000		
9	**Carrier three way valve**					
	V-0689					
	Valve angle (for non-bypass leg)	deg		90.000		
	Valve angle (for bypass leg)	deg		0.000		
10	**Daikin inlet valve**					
	V-0683					
	Valve angle	deg		0.000		
11	**Daikin chiller unit**					
	X-1401					
	Inlet temperature	℃	-	-		2
	Outlet temperature	℃	-	-		2

No	Description	Unit	Measured	Simulation	Error (%)	Note
	Total mass flow rate	kg/s	-	-		2
	Inlet pressure	kPa	-	-		2
	Outlet pressure	kPa	-	-		2
12	**Daikin outlet valve**					
	V-0684					
	Valve angle	deg		0.000		
13	**Daikin three-way valve**					
	V-0685					
	Valve angle (for non-bypass leg)	deg		0.000		
	Valve angle (for bypass leg)	deg		90.000		
14	**Chiller units water outlet**					
	150-06-WCCG-1069					
	Total temperature	℃		30.055		
	Total mass flow rate	kg/s		10.384		
	Static pressure	kPa		146.442		
15	**Fan coil unit supply**					
	50-06-WCCG-1101					
	Total temperature	℃		24.964		
	Total mass flow rate	kg/s		3.368		
	Static pressure	kPa		303.122		
16	**E-0620 inlet valve**					
	V-0677					
	Fraction open			1.000		
17	**Fan coil unit E-0620**					
	E-0620					
	Inlet temperature	℃		24.973		
	Outlet temperature	℃		25.802		
	Total mass flow rate	kg/s		1.128		
	Inlet pressure	kPa		263.497		
	Outlet pressure	kPa		262.859		
18	**E-0620 outlet valve**					
	V-0678					
	Fraction open			1.000		
19	**E-0619 inlet valve**					
	V-0679					
	Fraction open			1.000		
20	**Fan coil unit E-0619**					
	E-0619					
	Inlet temperature	℃		24.973		
	Outlet temperature	℃		25.811		
	Total mass flow rate	kg/s		1.116		
	Inlet pressure	kPa		263.754		
	Outlet pressure	kPa		262.950		
21	**E-0619 outlet valve**					
	V-0680					
	Fraction open			1.000		
22	**E-0618 inlet valve**					

No	Description	Unit	Measured	Simulation	Error (%)	Note
	V-0681					
	Fraction open			1.000		
23	**Fan coil unit E-0618**					
	E-0618					
	Inlet temperature	℃		24.973		
	Outlet temperature	℃		25.805		
	Total mass flow rate	kg/s		1.125		
	Inlet pressure	kPa		263.514		
	Outlet pressure	kPa		262.880		
24	**E-0618 outlet valve**					
	V-0682					
	Fraction open			1.000		
25	**Fan coil unit water outlet**					
	50-06-WCCG-1102					
	Total temperature	℃		25.815		
	Total mass flow rate	kg/s		3.368		
	Static pressure	kPa		222.999		
26	**Fan coil unit and chiller unit**					
	150-06-WCCG-1069					
	Total temperature	℃		29.080		
	Total mass flow rate	kg/s		13.752		
	Static pressure	kPa		222.614		

Note:

1. Discussed under Discussion – P-603.
2. No flow through P-0606.

4.4.4 Pool heat exchanger subsystem

For the pool heat exchanger subsystem, the inlet condition is specified by point 1, as depicted in **Figure 13**. The degree of the inlet valve opening is represented by designator 2. The flow conditions and pressure rise of the pump is given by designator 3. The outlet valve opening is represented by designator 4. The inlet condition of the pool heat exchanger is specified by point 5. Point 6 designates the fraction open of the control valve of the pool heat exchanger. Point 7 represents the flow conditions within the pool heat exchanger, with point 8 representing the outlet valve condition. Point 9 is the achieved exit flow results of the pool heat exchanger subsystem, with point 10 being the combined outlet flow of the chiller units, the fan coil units and the pool heat exchanger. All corresponding values are presented in **Table 23**.

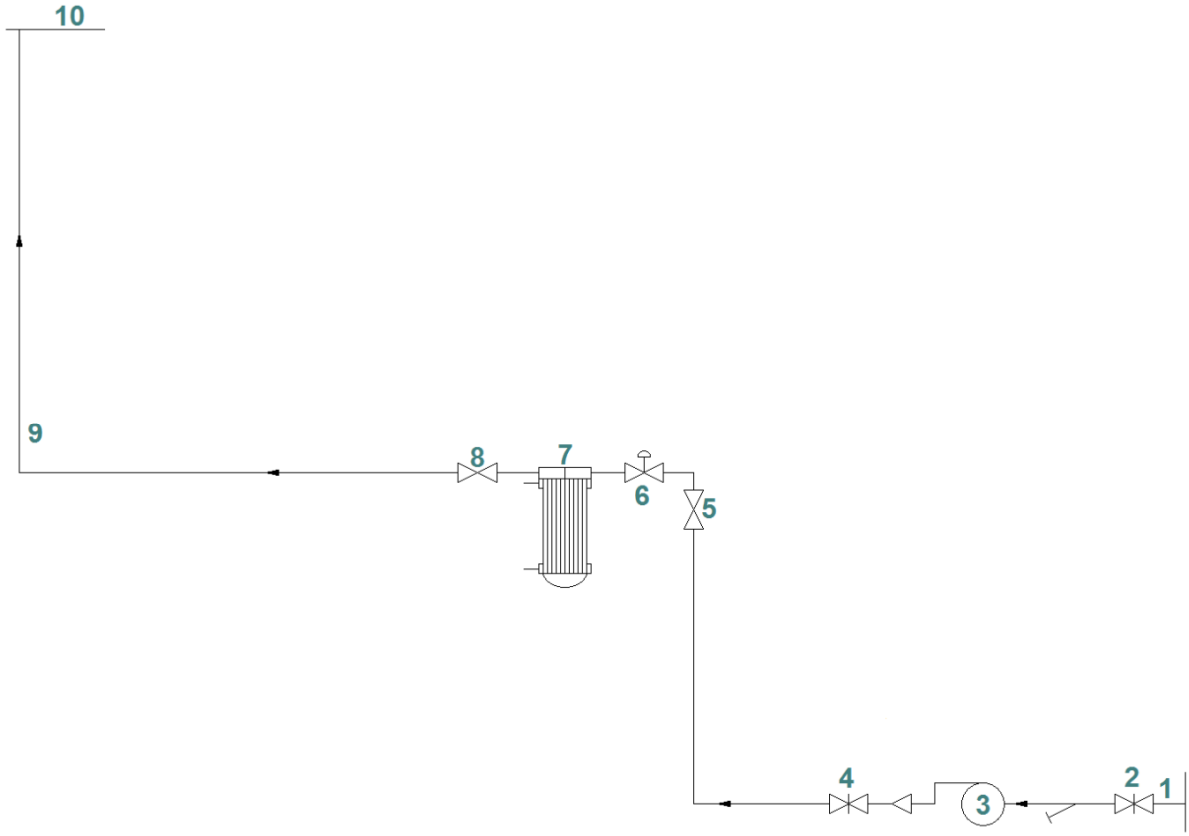

Figure 13: Pool heat exchanger subsystem

Table 23: Pool heat exchanger subsystem results

No	Description	Unit	Measured	Simulation	Error (%)	Note
1	**Pool heat exchanger**					
	200-06-WCCG-1051					
	Total temperature	℃		24.91		
	Total mass flow rate	kg/s		38.46		
	Static pressure	kPa		104.64		
2	**Pump P-0602 inlet valve**					
	V-0608					
	Valve angle	deg		90.00		
3	**Pump P-0602**					
	P-0602					
	Static temperature	℃		24.91		
	Total mass flow rate	kg/s		38.46		
	Inlet pressure	kPa	87.600	84.11	3.978	
	Outlet pressure	kPa	493.850	488.27	1.129	
4	**Pump P-0602 outlet valve**					
	V-0610					
	Valve angle	deg		90		
5	**HE-0301 inlet valve**					
	V-0614					
	Fraction open			1.00		
6	**HE-0301 control valve**					

No	Description	Unit	Measured	Simulation	Error (%)	Note
	TCV-0054					
	Fraction open			0.22		
7	**Pool heat exchanger**					
	E-0301					
	Inlet temperature (primary)	℃	33.000	33.00		1
	Outlet temperature (primary)	℃	31.750	28.51		1
	Total mass flow rate	kg/s	35.040	35.04		1
	Inlet pressure (primary)	kPa	219	219		1
	Outlet pressure (primary)	kPa	210	209.79	0.097	
	Inlet temperature	℃	24.200	25.11	3.746	
	Outlet temperature	℃	30.750	29.20	5.028	
	Total mass flow rate	kg/s		38.46		
	Inlet pressure (secondary)	kPa		277.14		
	Outlet pressure (secondary)	kPa		264.39		
8	**HE-0301 outlet valve**					
	V-0612					
	Fraction open			1.00		
9	**Pool heat exchanger room**					
	150-06-WCCG-1068					
	Total temperature	℃		29.20		
	Total mass flow rate	kg/s		38.46		
	Static pressure	kPa		241.54		
10	**Pool heat exchanger**					
	200-06-WCCG-1070					
	Total temperature	℃		29.160		
	Total mass flow rate	kg/s		52.221		
	Static pressure	kPa		213.97		

Note:

1. Used as input value.

4.4.5 Reactor heat exchanger subsystem

For the reactor heat exchanger subsystem, the inlet condition is specified by point 1, as depicted in **Figure 14**. The varying degrees of the inlet valve openings is represented by designators 2 to 5. The flow conditions within the heat exchangers are given from designators 6 to 9. The varying degrees of the outlet valve openings is represented by designators 10 to 13. All corresponding values are presented in **Table 24**.

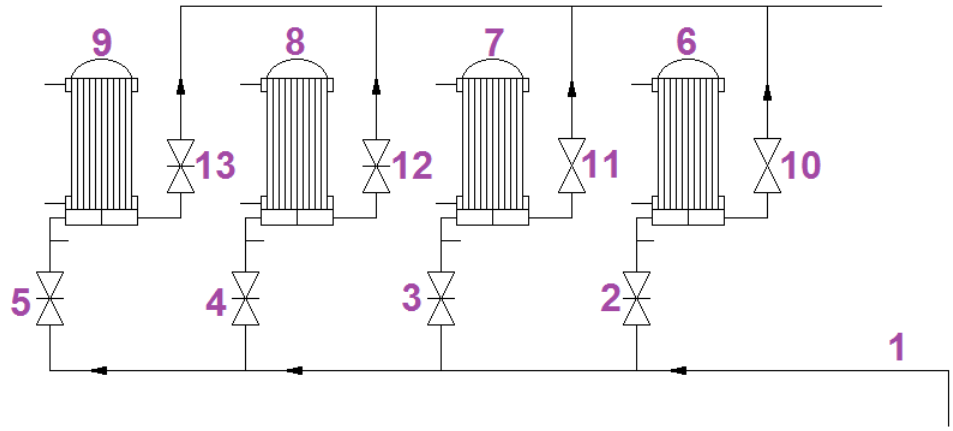

Figure 14: Reactor heat exchanger subsystem schematic

Table 24: Reactor heat exchanger subsystem results

No	Description	Unit	Measured	Simulation	Error (%)	Comments
1	**Reactor heat**					
	500-06-WCCG-1048					
	Total temperature	℃		24.974		
	Total mass flow rate	kg/s		564.969		
	Static pressure	kPa		281.827		
2	**E-0101 inlet valve**					
	V-0603					
	Valve angle	deg		90.000		
3	**E-0102 inlet valve**					
	V-0623					
	Valve angle	deg		90.000		
4	**E-0103 inlet valve**					
	V-0625					
	Valve angle	deg		90.000		
5	**E-0104 inlet valve**					
	V-0651					
	Valve angle	deg		90.000		

No	Description	Unit	Measured	Simulation	Error (%)	Comments
6	**Reactor heat**					
	E-0101					
	Inlet temperature	℃	44.500	44.500		1
	Outlet temperature	℃	37.500	37.447	0.141	
	Total mass flow rate	kg/s		137.466		
	Inlet pressure (primary)	kPa	418.000	418		
	Outlet pressure	kPa	365.500	397.324	8.707	
	Inlet temperature	℃	23.500	25.198	7.226	
	Outlet temperature	℃	31.000	31.364	1.174	
	Total mass flow rate	kg/s		157.324		
	Inlet pressure	kPa		256.426		
	Outlet pressure	kPa		240.308		
7	**Reactor heat**					
	E-0102					
	Inlet temperature	℃	45.000	45		1
	Outlet temperature	℃	39.000	39.024	0.062	
	Total mass flow rate	kg/s		170.653		
	Inlet pressure (primary)	kPa	424.500	424.5		1
	Outlet pressure	kPa	367.000	392.617	6.980	
	Inlet temperature	℃	24.000	25.180	4.917	
	Outlet temperature	℃	28.000	32.270	15.250	2
	Total mass flow rate	kg/s		143.983		
	Inlet pressure	kPa		257.168		
	Outlet pressure	kPa		242.081		
8	**Reactor heat**					
	E-0103					
	Inlet temperature	℃	44.500	44.5		1
	Outlet temperature	℃	38.000	37.953	0.124	
	Total mass flow rate	kg/s		146.363		
	Inlet pressure (primary)	kPa	403.000	403		1
	Outlet pressure	kPa	374.500	379.555	1.350	
	Inlet temperature	℃	23.500	25.175	7.128	
	Outlet temperature	℃	29.000	32.113	10.734	
	Total mass flow rate	kg/s		138.206		
	Inlet pressure	kPa		263.559		
	Outlet pressure	kPa		247.915		
9	**Reactor heat**					
	E-0104					
	Inlet temperature	℃	45.000	45		1
	Outlet temperature	℃	37.500	37.482	0.048	
	Total mass flow rate	kg/s		127.73		
	Inlet pressure (primary)	kPa	400.500	400.5		1
	Outlet pressure	kPa	367.000	382.604	4.252	
	Inlet temperature	℃	22.500	25.197	11.987	
	Outlet temperature	℃	31.000	31.909	2.932	
	Total mass flow rate	kg/s		143.285		
	Inlet pressure	kPa		252.802		

No	Description	Unit	Measured	Simulation	Error (%)	Comments
	Outlet pressure	kPa		240.697		
10	**E-0101 outlet valve**					
	V-0604					
	Fraction open			1.000		
11	**E-0102 outlet valve**					
	V-0624					
	Fraction open			1.000		
12	**E-0103 outlet valve**					
	V-0626					
	Valve angle	deg		90.000		
13	**E-0104 outlet valve**					
	V-0652					
	Valve angle	deg		90.000		

Note:

1. Used as input.
2. Addressed under Section 5.1.

4.4.6 Tube-cleaning subsystem

For the tube-cleaning subsystem, the outlet of the reactor heat exchanger subsystem is specified by point 1, as depicted in **Figure 15.** This forms the partial feed to the tube-cleaning subsystem denoted by 2. The fraction open of the inlet valve is represented by designator 3. The flow conditions and pressure rise of the pump is given by designator 4. Points 5 and 6 represent the valve fraction of the ball strainer's isolation valves. Numbers 7 to 14 refer to the relative isolation and inlet valves to the primary heat exchanger subsystem. Designators 15 to 18 point to fluid conditions into the respective reactor heat exchangers. All corresponding values are presented in **Table 25**.

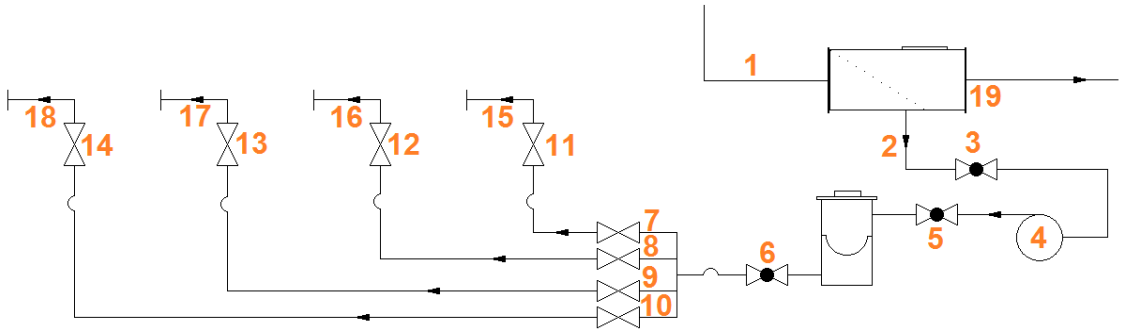

Figure 15: Tube-cleaning subsystem schematic

Table 25: Tube-cleaning subsystem results

No	Description	Unit	Measured	Simulation	Error (%)	Note
1	**Reactor heat exchanger room**					
	500-06-WCCG-1081					
	Total temperature	℃		31.901		
	Total mass flow rate	kg/s		582.798		
	Static pressure	kPa		224.941		
2	**Ball recirculation system inlet**					
	100-06-WCCG-1082					
	Total temperature	℃		31.902		
	Total mass flow rate	kg/s		17.828		
	Static pressure	kPa		238.821		
3	**P-0608 inlet valve**					
	TV-0001					
	Fraction open			1.000		
4	**Pump P-0608**					
	P-0608					
	Static temperature	℃		31.902		
	Total mass flow rate	kg/s		17.828		
	Inlet pressure	kPa		254.920		
	Outlet pressure	kPa		350.496		
5	**Ball collector inlet valve**					
	TV-0002					
	Fraction open			1.000		
6	**Ball collector outlet valve**					
	TV-0003					
	Fraction open			1.000		
7	**E-0104 circulation leg inlet**					
	TV-0007					
	Fraction open			1.000		
8	**E-0103 circulation leg inlet**					
	TV-0006					
	Fraction open			1.000		
9	**E-0102 circulation leg inlet**					
	TV-0005					
	Fraction open			1.000		
10	**E-0101 circulation leg inlet**					
	TV-0004					
	Fraction open			1.000		
11	**E-0104 circulation leg outlet**					
	TV-0008					
	Fraction open			1.000		
12	**E-0103 circulation leg outlet**					
	TV-0009					
	Fraction open			1.000		
13	**E-0102 circulation leg outlet**					
	TV-0010					
	Fraction open			1.000		

No	Description	Unit	Measured	Simulation	Error (%)	Note
14	**E-0101 circulation leg outlet**					
	TV-0011					
	Fraction open			1.000		
15	**E-0104 circulation leg outlet**					
	60-06-WCCG-1089					
	Total temperature	℃		31.939		
	Total mass flow rate	kg/s		4.578		
	Static pressure	kPa		251.860		
16	**E-0103 circulation leg outlet**					
	60-06-WCCG-1088					
	Total temperature	℃		31.939		
	Total mass flow rate	kg/s		3.973		
	Static pressure	kPa		262.848		
17	**E-0102 circulation leg outlet**					
	60-06-WCCG-1087					
	Total temperature	℃		31.939		
	Total mass flow rate	kg/s		4.238		
	Static pressure	kPa		256.359		
18	**E-0101 circulation leg outlet**					
	60-06-WCCG-1086					
	Total temperature	℃		31.072		
	Total mass flow rate	kg/s		4.914		
	Static pressure	kPa		258.019		
19	**Reactor heat exchanger**					
	500-06-WCCG-1057					
	Total temperature	℃		31.902		
	Total mass flow rate	kg/s	564.290	564.969	0.120	
	Static pressure	kPa		218.518		

5. Discussion

From the achieved results, it is clear that the model is representative of the actual system when considering the available data. However, this is not sufficient to fully validate the model, as the flow volumes in the relevant subsections are much larger in some than in others. Therefore, large differences in smaller subsections could easily be masked by the larger fluid volume of the system as a whole.

Factors that could potentially affect the model/received data are discussed below.

5.1 Calibration

An unlikely, but unavoidable factor that could affect the supplied data could be the calibration of the relevant measurement instrumentation. The disparity in the outlet temperatures of the secondary side of the primary heat exchangers (under the assumption that flow through the primary side is equally distributed) points to a potential calibration issue, because the values should have a smaller difference, as the heat exchangers are identical and the secondary side has virtually identical flow rates. This is affirmed by the fact that the inlet of the primary side is from a common source.

5.2 Pool heat exchanger (HE-0301)

A potential data error has been identified for HE-0301, where the available data from operational records is given in **Table 26**, which states the following (41):

Table 26: Pool heat exchanger flow conditions

Description	Unit	Absolute (Average)
Pool heat exchanger outlet pressure (primary)	kPa	297
Pool water flow (primary)	kg/s	35.04
Pool water delta temp (primary)	℃	2.25
Pool water inlet temp (primary)	℃	33.0
Pool heat exchanger secondary water inlet	℃	24.2
Pool heat exchanger secondary water outlet	℃	30.75
Pool-cooling water pump P-0602 inlet pressure	kPa	87.6
Pool-cooling water pump P-0602 outlet pressure	kPa	493.85

To determine the conflicting data, it is necessary to first calculate the required variables such as the flow rate. To determine the flow rate through the heat exchanger, the inlet and outlet pressure of the pool-cooling water pump P-0602 are used together with the relevant pump curve (70), which yields a flow rate of 38.88 kg/s.

As both systems (primary and secondary) operate in a single phase (liquid), the respective pressures of the systems are irrelevant when computing heat transfer.

It is known that the first law of thermodynamics applies where:

$$\dot{Q} = \dot{m}_c c_{pc}(T_{c,out} - T_{c,in}) \quad [22]$$

$$\dot{Q} = \dot{m}_h c_{ph}(T_{h,out} - T_{h,in}) \quad [23]$$

Where:

$\dot{Q}$	=	Heat transfer rate (kW)
$\dot{m}$	=	Mass flow rate (kg/s)
c_p	=	Constant pressure specific heat (kJ/kg.K)
T	=	Temperature (K)

From this, it can be stated (assuming c_{pc}= c_{ph}):

$$\dot{m}_c c_{pc}(T_{c,out} - T_{c,in}) = \dot{m}_h c_{ph}(T_{h,out} - T_{h,in}) \quad [24]$$

$$\dot{m}_c(T_{c,out} - T_{c,in} = \dot{m}_h(T_{h,out} - T_{h,in}) \quad [6]$$

$$38.88(30.75 - 24.2) = 35.04(33 - 30.75)$$

$$254.664 = 78.84?$$

From this, it can be clearly seen that some of the supplied data does not make sense, and it can therefore not be employed to verify the model.

5.3 Cooling tower nozzles

For the current model, the total flow rate through the cooling towers is the sum of the flow rates measured at FT-0601, the flow through pump P-0602 and the flow through pump P-0603. This means that the total flow of the model must be 617.19 kg/s. The

provided information states that there are 36 nozzles per cell. There are two cells per tower with three towers. Therefore, there are 216 nozzles in total. If the flow is equally distributed between the towers and cells, the flow rate per nozzle would be 2.85 kg/s or 2.924 l/s. This equates to 10.527 m^3/hr, which is below the minimum flow rates for the employed nozzle (No. 3), as seen in **Figure 16** (42).

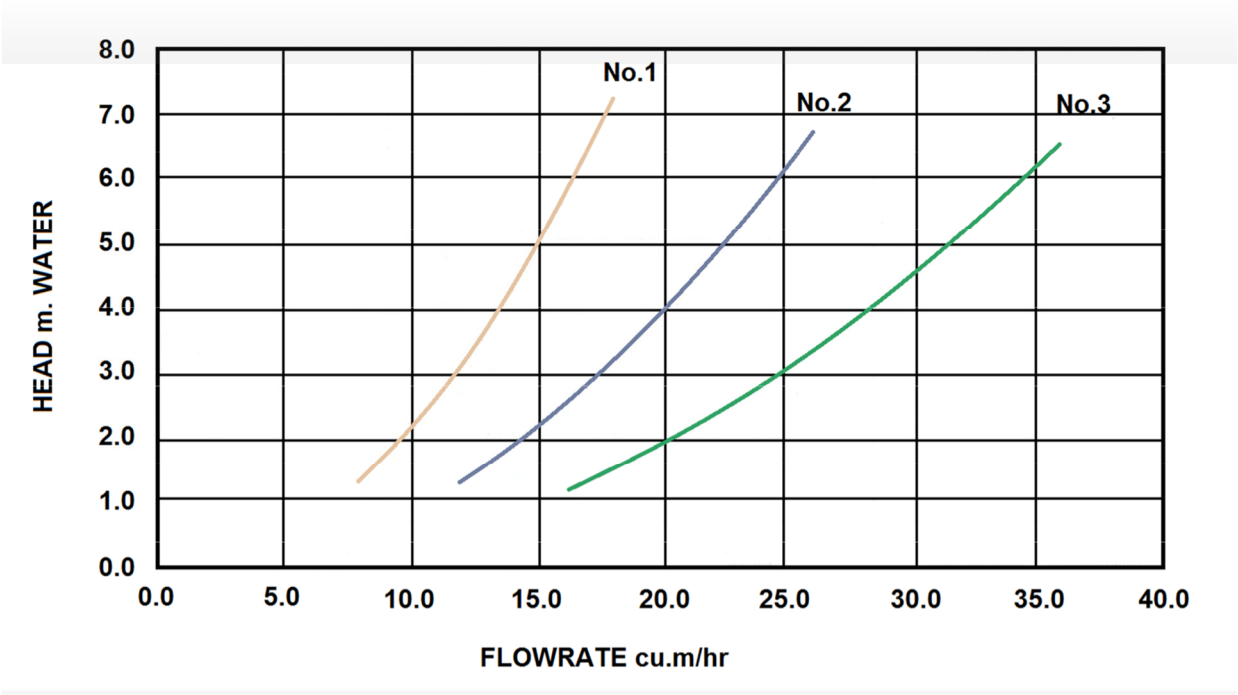

Figure 16: Nozzle calibration curves

If the flow is only circulated through two towers, the flow rate per nozzle increases to 15.79 cu.m/hr. This is still below the required flow rate for the nozzles to create a pressure differential large enough to facilitate effective atomisation of the droplets.

This is an area of concern if the data provided is correct. This would point to the severe under-utilisation of the cooling towers because the benefits of the larger surface area associated with improved atomisation are not exploited, which prompts the excessive use of the fans within the cooling towers.

As seen in the simulation model of the secondary cooling system, only the western and centre cooling towers' valves are configured to allow feed water to the tower to allow for adequate pressure head. It should be noted that the east and centre basins have an interconnecting level pipe, so the system feeds from all three basins.

5.4 Chiller and fan coil unit pump (P-603)

A potential discrepancy has been noted in the available data. The measurements supplied for verification of the chiller and fan coil unit's pump is given in **Table 27** (37).

Table 27: Chiller and fan coil unit's pump flow conditions

Description	Unit	Absolute (Average)
Chiller pump P-0603 outlet pressure	kPa	287.625

The chiller pump P-0603 outlet pressure with the given flow rate of 14.02 kg/s, when considering the relevant pump curve (71), yields an inlet pressure of 37.752 kPa (absolute), which is possible, albeit unlikely.

The NPSH for the pump is given as 1.74 m (17.064 kPa).

From this, one can calculate the minimum static pressure at the pump inlet to avoid cavitation by the following formula:

$$NPSH = P_S - P_{VAP} \quad [7]$$

From this, it is evident that the static pressure at the inlet of the pump has to be a minimum of:

$$P_S = NPSH + P_{VAP} = 17.064 + 3.011 = 20.075\ kPa$$

This, being possible, still raises the question of the original measurement's validity. The nearest pressure measurement is that of the pool-cooling water pump P-0602's inlet pressure at 87.6 kPa. Therefore, there has to be a significant pressure loss of 49.848 kPa. This could only point to inaccurate measurements or a blockage in the system, and if this is found to be so, it would most probably be in the Y-strainer Y-603.

6. Conclusion and recommendations

From the discussion above, it can be assumed that, with the available, albeit limited data, all crucial components, structures and systems have been identified and characterised. Due to the lack of sample input data, very specific conditions were imposed upon the model. It is therefore only a verified model. Due to the interdependency of the system and the potential of certain areas to mask the inaccuracies of others, the model would have to be validated at other set conditions prior to the use of this model at any other flow conditions. The current model does, however, allow for meaningful and relatively accurate analysis of the system as a whole.

The model suffers from the lack of comprehensive available data sets where all conditions are monitored and recorded at the same time. The available data is averaged over limited periods of operation. The status of subsystems and components over the same periods are unavailable. This yields a vastly averaged model that could not be entirely representative of the system.

However, in its current state, the model is accurate to within 10% of actual averaged values. It is therefore a useful addition to further analysis of the system. Further work would have to be performed with data sets in steady-state operating conditions at different power levels to fully validate the model.

Future work should include a fully integrated transient model with the primary loop, which gives a holistic view and expected latencies within the system under specific operating conditions. It also gives a more in-depth analysis of the cooling tower spray nozzles, which could be performed at master's degree level.

7. References

1. Versteeg, HK and Malalasekera, W. *An introduction to computational fluid dynamics – the finite volume method.* Harlow: Pearson Prentice Hall, 2007.

2. Glaser, A. *About the enrichment limit for research reactor conversion: why 20%?* (pp. 1–12). Boston, MA: Program on Science and Global Security, Princeton University, 2005.

3. McGraw-Hill. *Dictionary of engineering* (2nd edition). New York, NY: McGraw-Hill, 2003.

4. Meier, FA. *A P&ID standard: what, why, how?* Chapel Hill, NC: ISA Transactions (Vol. 41, pp. 389–394), 2002.

5. Dixon, SL. *Fluid mechanics, thermodynamics of turbomachinery* (5th edition). Amsterdam: Elsevier Butterworth Heinemann, 2005.

6. Çengel, Y. *Heat and mass transfer: a practical approach* (3rd edition). s.l.: McGraw-Hill, 2006.

7. Kloppers, JC. *User's manual wetcooling WCTPE – Wet Cooling Tower Performance Evaluation Software Version 2.0.* 2009.

8. Flownex Simulation Environment. *Flownex Library Manual.* 2012.

9. Rizzoni, G. *Principles and applications of electrical engineering.* Boston, MA: McGraw-Hill, 2000.

10. Vladimir, C, Heiliö, M, Krejic, N and Nedeljkov, M. *Mathematical model for efficient water flow management* (3rd edition, Vol. 11, pp. 1600–1612). s.l.: Elsevier, 2010.

11. Ortega, JM and Rheinboldt, WC. *Iterative solution of nonlinear equations in several variables.* Philadelphia, PA: Society for Industrial and Applied Mathematics, 2000.

12. NECSA. SAFARI-1 Reactor Trapogge system: ball catcher. Pelindaba: s.n., 2008.

13. Headley, MC. Guidelines for selecting the proper valve characteristics. *Valve Magazine,* Spring, Vol. 15(2), 2003.

14. Spirax Sarco. Check valves. International Site of Spirax Sarco. [Online] http://www.spiraxsarco.com/resources/steam-egnineering-tutorials/pipeline-ancillaries/check- valves.asp [cited: 20 May 2014].

15. Vlok, JWH. Reactor operations at SAFARI-1. Sydney: International Group

on Research Reactors (pp. 1–6), 9th Meeting of the International Group on Research Reactors, 2003.

16. Verbeek, P. Report on molybdenum-99 production for nuclear medicine – 2010–2020 (pp. 1–28). s.l.: Association of Imaging Producers & Equipment Suppliers, 2008.

17. World Nuclear News. South African radioisotope production on target, 17 September 2010. [Online] http://www.world-nuclear-news.org/RS-South_African_radioisotope_production_on_target-1709107.html [cited: 4 September 2012].

18. Sonntag, RE, Borgnakke, C and Van Wylen, GJ. *Fundamentals of thermodynamics.* s.l.: Wiley, 2003.

19. Vlok, JWH. SAFARI-1 research reactor safety analysis report. Reactor coolant systems and connected systems (Chapter 6). Pelindaba: s.n., 2010.

20. Janeschitz-Kriegl, J. *Thermo-hydraulic engineering using first principles (a data-oriented approach to thermal equipment design)* (Vol. 27, pp. 177–184). s.l.: Elsevier, 2007.

21. Kruger, JH and Du Toit, CG. *The simulation of a thermal-fluid system* (pp. 1–7). Melbourne: CSIRO, 2006.

22. Olivier, JC. *Network modelling of transient heat exchanger performance* (pp. 11–13). Potchefstroom: North-West University, 2005.

23. Flownex Simulation Environment. [Online] http://www.flownex.com/about-us/flownex- history.com.

24. White, FM. *Fluid mechanics.* Boston, MA: McGraw-Hill, 2003.

25. CD-Adapco. *User guide STAR CCM+ Version 6.02.007.* s.l.: CD-Adapco, 2011.

26. Kloppers, JC. Wetcooling software and consulting. Wetcooling, 2010. [Online] http://www.wetcooling.com/ [cited: 23 January 2013].

27. Kröger, DG. *Air-cooled heat exchangers and cooling towers thermal-flow performance, evaluation and design.* New York, NY: Begell House, 1998.

28. Howden Cooling Fans. *Howden cooling fans selection program CF-P20 Version 6.07* [Software program]. Hengelo: Howden Cooling Fans, 2010.

29. Sure Flow Equipment Inc. Custom engineered strainers. Sure Flow Equipment, 23 February 2010. [Online] http://www.sureflowequipment.com/custom-engineered/page7.cfm.

30. Gas Processors Suppliers Association. *Engineering data book FPS version volumes I & II sections 1-26.* Tulsa: Gas Processors Suppliers Association, 2004.

31. NECSA. *Electrical motor index.* Pelindaba: NECSA, 2012.

32. Du Plessis, K. Recommended heat fractions of pumps. *Personal Communication.* Pretoria: s.n., 2014.

33. Vasava, PR. *Fluid flow in T-junction of pipes.* Lappeenranta: Lappeenranta University of Technology, 2007.

34. Diaz, A and Van Der Walt, R. *PEL 90: the start-up of the SAFARI I research reactor.* Pelindaba: Atomic Energy Board, 1965.

35. KSB Pumps and Valves (Pty) Ltd. *Etabloc type series booklet 50 0p: close-coupled pumps.* Germiston: KSB Pumps and Valves, 2007.

36. Sure Flow Equipment Inc. *Y-strainers.* 2004.

37. Carrier. *Carrier reciprocating chiller rating.* Pelindaba: s.n., 2006.

38. AJM. *Carrier reciprocating chiller rating.* Pelindaba: AJM, 2006.

39. NECSA. Data sheet: induced draft cooling tower. Pretoria: NECSA, 1960.

40. COFIMCO S.p.A. Characteristics 5486-4-35N/33 M. Pelindaba: COFIMCO S.p.A., 1996.

41. NECSA. *SAFARI-1: secondary cooling water history.xls.* Pelindaba: s.n.

42. Unkown. *Spray nozzles for cooling towers: data.* s.l.: s.n.

43. NECSA. *SAFARI-1 research reactor: P&ID diagram.* Pelindaba: s.n.

44. NECSA. *Secondary cooling system piping ISO.* Pelindaba: s.n.

45. NECSA. *Data sheet: induced draft cooling tower.* Pelindaba: s.n., 1960.

46. NECSA. *Primary water flow FT-0001: 16/07/2011 to 11/04/2012.* Pelindaba: s.n., 2012.

47. NECSA. *Primary water flow FT-0002: 16/07/2011 to 11/04/2012.* Pelindaba: s.n., 2012.

48. NECSA. *Primary water flow FT-0003: 16/07/2011 to 11/04/2012.* Pelindaba: s.n., 2012.

49. NECSA. *Primary water inlet pressure: 16/07/2011 to 11/04/2012.* Pelindaba: s.n., 2012.

50. NECSA. *Primary heat exchanger E-0101 inlet pressure SS: 16/06/2011 to 11/04/2012*. Pelindaba: s.n., 2012.

51. NECSA. *Primary heat exchanger E-0102 outlet pressure SS: 16/06/2011 to 11/04/2012.* Pelindaba: s.n., 2012.

52. NECSA. *Primary heat exchanger E-0102 inlet pressure SS: 16/06/2011 to 11/04/2012.* Pelindaba: s.n., 2012.

53. NECSA. *Primary heat exchanger E-0101 outlet pressure SS: 16/06/2011 to 11/04/2012.* Pelindaba: s.n., 2012.

54. NECSA. *Primary heat exchanger E-0103 inlet pressure SS: 16/06/2011 to 11/04/2012.* Pelindaba: s.n., 2012.

55. NECSA. *Primary heat exchanger E-0104 outlet pressure SS: 16/06/2011 to 11/04/2012.* Pelindaba: s.n., 2012.

56. NECSA. *Primary heat exchanger E-0104 inlet pressure SS:* 16/06/2011 to 11/04/2012. Pelindaba: s.n., 2012.

57. NECSA. *Primary heat exchanger E-0101 inlet temperature SS: 16/06/2011 to 11/04/2012.* Pelindaba: s.n., 2012.

58. NECSA. *Primary heat exchanger E-0101 inlet temperature SS: 16/06/2011 to 11/04/2012.* Pelindaba: s.n., 2012.

59. NECSA. *Primary heat exchanger E-0101 inlet temperature SS: 16/06/2011 to 11/04/2012.* Pelindaba: s.n., 2012.

60. NECSA. *Primary heat exchanger E-0101 outlet temperature SS: 16/06/2011 to 11/04/2012.* Pelindaba: s.n., 2012.

61. NECSA. *Primary heat exchanger E-0102 inlet temperature SS: 16/06/2011 to 11/04/2012.* Pelindaba: s.n., 2012.

62. NECSA. *Primary heat exchanger E-0103 outlet temperature TS: 16/06/2011 to 11/04/2012.* Pelindaba: s.n., 2012.

63. NECSA. *Primary heat exchanger E-0101 outlet temperature SS: 16/06/2011 to 11/04/2012.* Pelindaba: s.n., 2012.

64. NECSA. *Primary heat exchanger E-0103 inlet temperature SS: 16/06/2011 to 11/04/2012.* Pelindaba: s.n., 2012.

65. NECSA. *Primary heat exchanger E-0104 outlet temperature SS: 16/06/2011 to 11/04/2012.* Pelindaba: s.n., 2012.

66. NECSA. *Primary Heat exchanger E-0104 inlet temperature SS: 16/06/2011 to 11/04/2012.* Pelindaba: s.n., 2012.

67. AEC-AEK. *Orifice plate. Reactor secondary flow.* Pelindaba: AEC-AEK, 1997.

68. NECSA. *Estimated performance curve: Harland SNC 3 – reduced Imp. 1450 RPM.* Pelindaba: s.n.

69. NECSA. *Electrical motor index.* Pelindaba: s.n., 2009.

70. Weir Minerals Africa. *Uniglide pump curve: SDC100-125A rev 0.* Johannesburg: Weir Minerals Africa, 2012.

71. NECSA. *Monoglide pump curve: SNC3.* Johannesburg: Weir Minerals Africa, 2010.

72. Carrier. *30HZ 043-280 reciprocating liquid chillers.* Montluel: Carrier SA, 1997.

73. CRANE CO. *E-101 OM specifications.* New York, NY: s.n., 1962.

74. ALLIS-CHALMERS. *E-101 OM specifications.* Washington, DC: s.n., 1960.

75. CRANE CO. *E-301 OM specifications.* New York, NY: s.n., 1962.

76. ALLIS-CHALMERS. *E-301 OM specifications.* Washington, DC: s.n., 1960.

77. Airtec Engineering Co. *16'-0" x 3'-0" Dia heat exchanger tube sheet and baffle details.* Johannesburg: Airtec Engineering Co., 1971.

78. CRANE CO. *Construction details 20 1/4" I.D. Horizontal pool heat exchanger. Hall, Longmore & Co., LTD.* New York, NY: CRANE CO., 1962.

79. NECSA. *Tube layout 20 1/4" I.D. Horizontal pool heat exchanger. Hall, Longmore & Co., LTD.* New York, NY: CRANE CO., 1962.

80. NECSA. *20 1/4" I.D. Horizontal pool heat exchanger. Hall, Longmore & Co., LTD.* New York, NY: CRANCE CO., 1962.

81. NECSA. *26 1/4" I.D. Horizontal primary heat exchanger. Hall, Longmore & Co., LTD.* New York, NY: CRANE CO., 1962.

82. NECSA. *Pool water flow FT-0301: 16/07/2011 to 11/04/2012.* Pelindaba: s.n., 2012.

83. NECSA. *Pool water delta temperature: 16/07/2011 to 11/04/2012.* Pelindaba: s.n., 2012.

84. NECSA. *Pool water inlet temperature: 16/07/2011 to 11/04/2012.* Pelindaba: s.n., 2012.

85. NECSA. *Primary heat exchanger E-0101 inlet temperature TS: 16/06/2011 to 11/04/2012.* Pelindaba: s.n., 2012.

86. NECSA. *Primary heat exchanger E-0101 inlet temperature TS: 16/06/2011 to 11/04/2012.* Pelindaba: s.n., 2012.

87. NECSA. *Primary heat exchanger E-0102 inlet temperature TS: 16/06/2011 to 11/04/2012.* Pelindaba: s.n., 2012.

88. NECSA. *Primary heat exchanger E-0102 outlet temperature TS: 16/06/2011 to 11/04/2012.* Pelindaba: s.n., 2012.

89. NECSA. *Primary heat exchanger E-0103 inlet temperature TS: 16/06/2011 to 11/04/2012.* Pelindaba: s.n., 2012.

90. NECSA. *Primary heat exchanger E-0103 outlet temperature TS: 16/06/2011 to 11/04/2012.* Pelindaba: s.n., 2012.

91. NECSA. *Primary heat exchanger E-0104 inlet temperature TS: 16/06/2011 to 11/04/2012.* Pelindaba: s.n., 2012.

92. NECSA. *Primary heat exchanger E-0104 outlet temperature TS: 16/06/2011 to 11/04/2012.* Pelindaba: s.n., 2012.

93. NECSA. *Equipment numbers.* Pelindaba: s.n., 2009.

94. NECSA. *Ambient dry bulb temperature: measurements 16/06/2011 to 11/04/2012.* Pelindaba: s.n., 2012.

95. NECSA. Ambient wet bulb temperature: measurements 16/06/2011 to 11/04/2012. Pelindaba : s.n., 2012.

96. PECI. The PECI functional testing guide: fundamentals to the field Version 2. *PECI.* September 2006. [Online] http://www.peci.org/ftguide/ftg/SystemModules/AirHandlers/AHU_ReferenceGuide/FTG_Chapters/ Chapter_10_Fans_and_Drives.htm [cited: 6 November 2012].

97. HOLST & CO. LTD. *Cooling tower general arrangement.* Watford: HOLST & CO. LTD, 1962.